UNIVERSITÀ DEGLI STUDI DI MILANO

DOCTORAL PROGRAMME IN TRANSLATIONAL MEDICINE (XXXVIII CYCLE)
DEPARTMENT OF PATHOPHYSIOLOGY AND TRANSPLANTATION

DOCTORAL THESIS

Ultra-low level soluble p24 is associated with inflammation in people with HIV on long-term virologically suppressive antiretroviral therapy

Scientific-disciplinary sector: MEDS-10/B – Infectious Diseases

Ph.D. candidate: Matteo Augello
Student ID: R13876
ORCID: 0000-0002-1031-9504

Tutor: Prof. Camilla Tincati

Doctoral programme coordinator: Prof. Mario Salvatore Clerici

Academic year 2024/2025

Index

1. Abstract

1.1. Introduction

Despite virologically suppressive antiretroviral therapy (ART), residual inflammation persists in people with HIV (PWH), thus driving higher risk of serious non-AIDS events (SNAEs) and mortality. Circulating HIV proteins have been detected in some suppressed PWH, as an expression of the persistence of the translation-competent reservoir. We therefore seek to investigate whether peripheral inflammation and mortality risk are associated with p24 production in this population.

1.2. Methods

PWH on suppressive ART and age/sex-matched healthy controls without HIV were enrolled. Ultra-low level serum p24 was cross-sectionally (baseline) and longitudinally (6 and 12 months) quantified by Simoa following immune complexes dissociation. In addition, the following were cross-sectionally measured at baseline: plasma biomarkers of inflammaging (Luminex/ELISA), CD38+CD8+ T-cells (flow cytometry), cell-associated total/unintegrated/integrated HIV DNA (qPCR). Mortality risk was estimated by VACS Index 2.0. *In vitro* experiments tested whether p24 modulates IP-10 secretion by PBMCs.

1.3. Results

120 PWH and 20 controls were recruited. PWH exhibited a distinct inflammaging profile characterised by elevated IP-10, TNF-α, IL-17A, IL-8, sCD14, sCD163, TIMP-1, and GDF-15 compared to controls. Several biomarkers were associated with the VACS Index 2.0 in univariable analyses, but only IP-10 and GDF-15 remained independently associated in multivariable modelling. Soluble p24 was detectable in 25/120 (20.8%) PWH at baseline (median: 0.0516 pg/mL; range: 0.0264–0.8280 pg/mL), and its detectability was associated with male sex yet not with immunological parameters or HIV DNA. Among inflammaging biomarkers, p24 was associated exclusively with higher plasma IP-10, both as categorical and continuous variable, even after adjustment for sex, age, CD4 T-cell count, and ART duration. Longitudinal analyses in a subset of 30 PWH revealed dynamic p24 patterns, with persistently p24-

positive PWH exhibiting the highest baseline IP-10 levels. *In vitro*, p24 alone did not induce IP-10 secretion, but in the presence of IFN-γ and TNF-α, it produced a modest yet significant increase, supporting a context-dependent proinflammatory effect.

1.4. Conclusions

These findings demonstrate that a subset (~21%) of virologically suppressed PWH produce detectable levels of soluble p24, and that this residual HIV protein expression is selectively associated with heightened IP-10–mediated inflammation. Given the positive association between IP-10 and VACS Index 2.0, a measure of physiologic frailty and risk of death, these data suggest that p24-driven inflammation may contribute to SNAEs and mortality in virologically suppressed PWH.

2. Introduction

2.1. Inflammaging and serious non-AIDS events in people with HIV despite effective antiretroviral therapy

Antiretroviral therapy (ART) has substantially modified the natural history of human immunodeficiency virus (HIV) infection, by significantly reducing morbidity and mortality related to acquired immune deficiency syndrome (AIDS) (1). Consequently, HIV infection has shifted from being a fatal illness to a chronic, manageable condition. This paradigm shift is attributable to the effective suppression of viral replication by potent antiretroviral drugs, which in turn enables the repletion of CD4 T-cell counts (2).

However, despite virologically effective ART, people with HIV (PWH) continue to experience residual inflammation and chronic immune activation, a pattern that fails to return to the levels seen in the general population of similar age (3-8). This chronic, low-grade inflammatory state combined with immune activation resembles the age-associated phenomenon termed "inflammaging" and appears to accelerate biologic ageing in ART-treated PWH, producing an immune profile similar to that seen in the elderly. These processes drive an increased risk of serious non-AIDS events (SNAEs) – including cardiovascular diseases, non-AIDS malignancies, renal and hepatic dysfunction, bone disease, and neurocognitive impairment – as well as all-cause mortality compared to the general population of similar age (9-15).

Since SNAEs account for the majority of HIV-related morbidity and mortality in the ART era, research has shifted toward interventions that target inflammation and traditional risk factors in PWH (16). Early ART initiation, particularly when CD4 T-cell counts are above 500 cells/μL, significantly reduces the risk of SNAEs and mortality (17), by decreasing the residual immune imbalances. Recent studies testing anti-inflammatory approaches and statin therapy (e.g., pitavastatin in the REPRIEVE trial) have shown promise for lowering the risk of cardiovascular events in PWH (18), supporting the idea that adjunctive therapies that blunt residual inflammation may translate into meaningful clinical benefit in this setting.

2.2. The VACS Index as a predictor of mortality in people with HIV

The Veterans Aging Cohort Study (VACS) Index has been developed to provide a more precise assessment of health outcomes in PWH, in which multiorgan dysfunction and physiological frailty consequent to persistent inflammaging is not adequately represented by traditional HIV markers such as CD4 T-cell count and HIV RNA levels (19). The VACS Index integrates age with eight routinely measured clinical parameters: CD4 T-cell count, HIV RNA, haemoglobin, aspartate aminotransferase (AST), alanine aminotransferase (ALT), platelet count, creatinine and HCV serostatus. This composite index, originally developed in United States (US) veterans and then validated in independent cohorts from both the US and Europe, has demonstrated superior predictive accuracy for all-cause mortality in ART-treated PWH compared to an index restricted to CD4 T-cell count, HIV RNA and age, with consistent performances across demographic subgroups and clinical contexts (20). Importantly, the VACS Index also shows strong correlations with IL-6, D-dimer, and sCD14, highlighting the link between inflammation and adverse outcomes, including multiorgan dysfunction, physiologic frailty, and mortality, among PWH (21).

The VACS Index 2.0 enhanced the predictive accuracy of the original score by adding other non–HIV-specific clinical biomarkers, including albumin, white blood cell count and body mass index (BMI) (22). It has been shown to predict a wide range of adverse outcomes in PWH, such as all-cause (23) and cause-specific (24) mortality, hospitalisation (25), as well as functional decline (26). In the context of cause-specific mortality, the VACS Index 2.0 exhibits its highest predictive performance for deaths attributable to AIDS, liver disease, and respiratory infections, whereas its discriminatory capacity for cardiovascular-related mortality remains comparatively limited (24). Enhancing discrimination for cardiovascular-related mortality may require further refinement of the VACS Index 2.0, potentially through the incorporation of additional biomarkers such as lipid profiles, which provide established indicators of cardiovascular health.

2.3. Pathogenesis of inflammaging in people with HIV

Multiple mechanisms have been proposed to contribute to the HIV-associated inflammaging, including the persistence of viral reservoirs despite effective ART, residual viral replication, microbial translocation, and coinfections (27).

Latently infected memory CD4 T cells and tissue-resident macrophages can harbour integrated HIV DNA (28, 29). Although frequently defective and therefore incapable of producing infectious virions, these proviruses may still generate viral RNAs or proteins, which act as continuous sources of antigenic stimulation and immune activation (30). Furthermore, residual low-level HIV replication is thought to persist in anatomical sites where antiretroviral drug penetration is limited, such as lymphatic tissues (31, 32): within these sanctuaries, ongoing cycles of infection and replenishment of the latent reservoir can occur, thereby sustaining chronic immune stimulation (33).

Another critical contributor to the HIV-associated inflammaging is microbial translocation. HIV infection leads to structural and functional damage of the gut mucosal barrier, characterised by the depletion of Th17 and Th22 cell subsets and a disruption of epithelial integrity. As a consequence, microbial products such as lipopolysaccharide, (1→3)-β-D-glucan, and other pathogen-associated molecular patterns can translocate into the systemic circulation. This process drives the activation of innate immune cells, including monocytes, and promotes the release of pro-inflammatory mediators such as IL-6 and TNF-α, thereby sustaining chronic immune activation (34, 35).

In addition, concomitant infections, such as those sustained by hepatitis viruses (36, 37) and *Mycobacterium tuberculosis* (38), as well as latent chronic viral coinfections, including cytomegalovirus and other herpesviruses (39), contribute to the maintenance of a persistent antigenic burden. This persistent immune stimulation promotes sustained T-cell activation, elevated production of pro-inflammatory cytokines, and progressive immune exhaustion, thereby amplifying the chronic inflammatory *milieu* associated with HIV infection (36-39).

2.4. Transcriptionally and translationally competent HIV reservoir and inflammation

HIV structural and non-structural proteins – including p24, gp120, Nef, and Tat – have been found in plasma or serum (40-47), as well as in PBMCs (48-52) and tissues (46, 53, 54) of some PWH on virologically suppressive ART. This protein production reflects ongoing expression from persistent HIV proviruses despite ART, which is not able to suppress proviral gene expression (30, 55, 56). Although the majority of these proviruses are defective, i.e. characterised by large internal deletions and hypermutations, and thus unable to encode replication-competent viruses (30, 55), they can be still transcribed into RNAs and thus translated into proteins (30, 50, 56-61).

The enduring production of HIV transcripts and proteins in the absence of viral replication on long-term ART has been associated with heightened inflammation. More specifically, both cell-associated HIV RNA – a measure of HIV transcription – and antibody responses to specific HIV proteins – which serves as a surrogate marker for the presence of viral proteins *in vivo* – have been found positively associated with plasma D-dimer, a marker of systemic inflammation (58, 59). Furthermore, the presence of soluble gp120 in the plasma of virologically suppressed PWH has been reported to associate with increased levels of the pro-inflammatory cytokine IL-6 (44). The ability of both HIV transcripts and proteins to induce innate immune activation and production of pro-inflammatory cytokines/chemokines has also been confirmed in *in vitro* models (62-72).

3. Rationale and aims of the study

Despite the virological efficacy of ART, PWH continue to experience chronic immune activation and residual inflammation, a condition reminiscent of accelerated aging, often referred to as “inflammaging”. This persistent inflammatory state is strongly associated with an increased risk of SNAEs and mortality, representing a major determinant of long-term health outcomes in virologically suppressed PWH. Among the multiple factors implicated in sustaining inflammaging, residual HIV expression at the transcriptional and protein level has emerged as a plausible contributor. Previous studies have shown that HIV structural and non-structural proteins may be detectable in plasma and tissues of individuals on effective ART, reflecting the activity of translationally competent proviruses. These viral products have been suggested to directly or indirectly drive immune activation, yet the biological and clinical relevance of such residual protein production remains incompletely understood.

In particular, HIV p24 is a 24-kDa protein encoded by the *gag* gene and constitute the main structural component of the viral capsid. Each HIV particle contains approximately 2,000 p24 molecules, making it the most abundant viral antigen (73). During acute HIV infection, the virus replicates exponentially, leading to the appearance of detectable p24 in blood, which strongly correlates with HIV RNA (74). After seroconversion, the development of anti-p24 antibodies makes the detection of p24 inaccurate by immunoassays due to the formation of antigen-antibody immune complexes (75). Sample pre-processing methods that enable immune complex dissociation – such as heat-mediated (76) or acid (77) dissociation – are therefore required to detect p24 beyond the acute phase of HIV infection. Early studies showed that, in ART-naïve people with chronic HIV infection, p24 detectability is associated with a higher risk of developing AIDS (78-81). Furthermore, plasma p24 quantification has been reported in some studies to outperform HIV RNA measurement in predicting CD4 T-cell decline (80, 82) and, in another study, to correlate more strongly with CD8 T-cell activation (83). More recently, plasma p24 has also been associated with higher levels of D-dimer and IFN-α in individuals with chronic HIV infection prior to ART start (40). However, whether circulating p24 may

be associated with persistent inflammation or immune activation in PWH on virologically suppressive ART is currently unknown.

The present study was therefore designed to investigate whether residual HIV protein expression, as measured by soluble p24 detectability in serum, contributes to the inflammaging profile of virologically suppressed PWH. In detail, the specific aims of the study were:

1. To characterise the inflammaging *milieu* of PWH on long-term ART in comparison with people without HIV (PWoH), through the measurement of a panel of plasma biomarkers;
2. To examine the association between inflammaging biomarkers and mortality risk, as estimated by the VACS Index 2.0, in order to identify the most relevant mediators of adverse outcomes;
3. To determine the prevalence and dynamics of soluble p24 detectability in virologically suppressed PWH using an ultrasensitive assay;
4. To explore the relationship between soluble p24 and inflammaging biomarkers, and to validate observed associations through *in vitro* experiments;
5. To assess whether residual p24 production is associated with the size of viral reservoir or residual viral replication.

4. Methods

4.1. Study design and population

In this cross-sectional study, PWH on long-term virologically suppressive (HIV RNA <20 copies/mL for at least 5 years) ART were consecutively enrolled at the Clinic of Infectious Diseases and Tropical Medicine, San Paolo Hospital, ASST Santi Paolo e Carlo, Department of Health Sciences, University of Milan, Milan, Italy. Age- and sex-matched healthy PWoH were also recruited as controls.

Peripheral blood was collected from all participants in EDTA tubes and serum tubes by venipuncture. Plasma and serum were separated by centrifugation and stored at –80°C until subsequent analysis. Whole blood was used immediately.

For a subset of PWH, longitudinal serum samples were available at two further time points in addition to baseline (T0), i.e. at 6 months (T1) and 12 months (T2).

Demographic, clinical and HIV-related characteristics were retrieved from electronic medical records. Physiological frailty and risk of mortality in PWH were estimated by the VACS Index 2.0 as previously reported (22-24), using an online calculator (https://www.mdcalc.com/calc/10402/veterans-aging-cohort-study-vacs-2.0-index).

The study was approved by the institutional Ethics Committee. All the research was conducted in accordance with the Declaration of Helsinki.

4.2. Soluble biomarkers of inflammaging

Soluble biomarkers of inflammation [interferon γ-induced protein 10 (IP-10), tumour necrosis factor α (TNF-α), interleukin 6 (IL-6), interleukin 8 (IL-8), interleukin 17A (IL-17A)], monocyte activation [soluble CD14 (sCD14), soluble CD163 (sCD163)], senescence [tissue inhibitor of metalloproteinases 1 (TIMP-1), growth differentiation factor 15 (GDF-15)], and immunomodulatory cytokines [interleukin 2 (IL-2), interleukin 4 (IL-4)] were cross-sectionally quantified in plasma of PWH and PWoH by Luminex® technology using the FLEXMAP 3D® System, and analysed using Bio-Plex® Manager Software 6.0. The following Luminex® panels were used: IL-2, IL-4, IL-6, IL-8, TNF-α (high sensitivity 5-plex); IP-10, IL-17A, sCD163, GDF-15 (4-plex); sCD14 (1-plex); TIMP-1 (1-plex). Plasma samples presenting biomarkers below the limit of detection were adjusted to 0.

Reactive oxygen species modulator 1 (ROMO1) – a marker of mitochondrial oxidative stress – was cross-sectionally quantified in plasma of PWH and PWoH by ELISA [Abbexa® Human Reactive Oxygen Species Modulator 1 (ROMO1) ELISA Kit] according to the manufacturer's instructions. The optical density was measured by using PerkinElmer EnSight™ Multimode Plate Reader, and results computed with GraphPad Prism 10.

4.3. Activated CD8 T cells

Activated CD8 T cells (CD8+CD38+ cells) were cross-sectionally quantified on fresh whole blood of PWH by flow cytometry. Briefly, samples were prepared with the automated BD FACSDuet™ Sample Preparation System by mixing 50 µL of fresh whole blood and 40 µL of fluorescently-labelled antibodies cocktail (CD45–V500, CD4–APC-Cy7, CD8–PerCP-Cy5.5, CD38–APC) in BD Trucount™ Tubes. After a 20-minute incubation at room temperature, red blood cells were lysed with BD FACS™ Lysing Solution. Samples were then acquired on a BD FACSLyric™ Flow Cytometry System, and fcs files analysed with BD FACSuite™ Clinical Application software. The gating strategy for a representative sample is shown in the **Supplementary material** (**Figure S1**).

4.4. Soluble p24

Ultra-low level soluble HIV capsid protein p24 was quantified in serum both cross-sectionally (in all PWH) and longitudinally (in a subset of PWH with available longitudinal samples) by means of digital single-molecule array (Simoa). The Simoa® HIV p24 Advantage Kit on a Quanterix® SR-X® Biomarker Detection System was used according to the manufacturer's instructions.

Since following seroconversion host anti-HIV antibodies form immune complexes with HIV p24 – therefore interfering with its detection by immunoassays (75) –, serum samples were subjected to acid pre-treatment with the ZeptoMetrix® RETROTEK™ HIV-1 p24 ICx/CRx kit before running the assay in order to induce immune complexes dissociation (ICD), thus improving the assay sensitivity as previously reported (40). Briefly, after a 60-minute thawing at room temperature, serum samples were thoroughly mixed and then centrifuged at 10,000 g for 5 minutes to remove debris.

Serum was incubated for 1 hour at 37°C after adding the acid (ICx Acid Reagent) at 1:1 ratio, and then the reaction was quenched by adding the base (The ICx Base Reagent) at 1:1 ratio. Since at the end of the process the serum sample was 1:3 diluted, results obtained from the p24 quantification were multiplied ×3. Our exploratory experiments showed that the acid pre-treatment was able to significantly increase both the serum p24 levels and the detectability rate above the limit of detection (LOD) specified in the assay data sheet (0.0045 pg/mL) (**Figure S2, Supplementary material**).

To determine the background signal, HIV-1 p24 was also measured in serum of PWoH with the same assay and following the same acid pre-treatment process, and the positivity cut-off set at 3 standard deviations (SD) from the mean.

4.5. Cell-associated HIV DNA

Cell-associated total, unintegrated, and integrated HIV DNA was quantified as previously described (84, 85).

Cellular DNA was isolated from a pellet of different amounts of PBMCs by a DNA extraction kit (QIAGEN QIAamp Blood Mini kit) following the manufacturers' instructions. The concentration and quality of the isolated DNA were determined using the NanoVue Plus spectrophotometer (GE Healthcare) and the absorbance ratios of 260/280 and 260/230 were used to control the purity of the samples: all samples had a ratio of about 1.8 and 2.0 respectively, and are accepted as "pure" DNA.

Unintegrated HIV DNA (uDNA) (i.e., the ensemble of extrachromosomal viral DNA forms, including both linear cDNA and all the closed circular 1-LTR and 2-LTR and other rearranged forms) was obtained from cellular DNA by an optimized chromatographic procedure that separates high molecular weight DNA from low molecular weight DNA. The uDNA was present in the eluate fraction (86).

Total and unintegrated HIV DNA were simultaneously analysed by a SYBR Green qPCR based method [TotUFsys qPCR platform; LOD and limit of quantification (LOQ): 1 copy and 2 copies/1.5×10^5 cells, respectively] in a single run using a single set of specific primers selected in the 5' LTR-Gag region of the HIV-1 genome, including the highly conserved primer-binding site (PBS); this method could detect all HIV-1 subtypes in the M group. Amplification, data acquisition and analysis were

carried out using an Applied Biosystems 7500 Real-Time PCR instrument with the Sequence Detection System software package (version 1.4.0). The fluorescence intensity of the products was measured at the end of each cycle and post-PCR melt curve analysis was performed to detect primer-dimers or other non-specific products and to confirm the specificity of the target. Each sample was analysed in two or six replicates, consisting of one or three wells containing 0.5 µg of DNA or the equivalent quantity of elution fraction and one or three wells containing 1.0 µg of DNA or the equivalent quantity of elution fraction (1.5 µg or 4.5 µg of DNA to ensure the detection of the target even in low copy numbers, i.e., near the LOQ). For samples with HIV DNA datum quantified near or detected below LOQ, one or two additional 1 µg replicates were tested for a total of 6.5 (or 5.5) µg of DNA (~10^6 PBMCs). In the case of negative amplification, a PCR spike test was performed by adding two or ten copies of plasmid standard to the samples to exclude the presence of inhibitors.

The HIV DNA copy number was quantified by interpolating the experimentally determined cycle threshold (Ct) based on standard curves generated using half-log serial dilutions from 10^5 to 2 copies (setting the quantification limits at 2 copies/PCR) and by adding up the copy number from the 0.5 and 1.0 µg replicates and expressed as copies/µg. The amount of integrated HIV DNA (iDNA) was obtained by subtracting the amount of uDNA from the amount of total HIV DNA (tDNA).

For the accurate enumeration of the analysed cells in qPCR, the single copy housekeeping Rpp40 gene was amplified. This approach provided a control for cellular DNA degradation, presence of PCR inhibitors and input DNA normalization. The standard curve for the quantification of a 100 bp fragment of the Rpp40 gene was made with 10- and 2-fold serial dilutions of a reference human genomic DNA (Promega) ranging from 100 to 0.01 ng, assuming 7.0 pg of DNA content per human diploid genome as conversion factor (http://www.genomesize.com). The data were then expressed as copies/10^6 PBMCs.

4.6. In vitro stimulation of PBMCs with p24 and IP-10 quantification in supernatant

Cryopreserved PBMCs from PWoH were thawed and then rested for 4 hours in Roswell Park Memorial Institute (RPMI) 1640 medium supplemented with 10% foetal bovine serum (FBS), 1% glutamine, and 1% penicillin/streptomycin at 37 °C in a

humidified 5% CO_2 atmosphere. After resting, viable PBMCs were plated at a density of 2×10^5 per well (200 µL, corresponding to a concentration of 1×10^6 PBMCs/mL) in 96-well plates in culture medium consisting of RPMI 1640 supplemented with 10% human serum, 1% glutamine, and 1% penicillin/streptomycin, and stimulated according to the experimental design. Endotoxin-free recombinant p24 protein [ACROBiosystems HIV (HIV1-HXB2) capsid protein p24, His Tag, cat. #CP4-H52H3] was tested in duplicate at four serial dilutions (100 ng/mL, 10 ng/mL, 1 ng/mL, 0.1 ng/mL), alongside an unstimulated control, either alone or in the presence of both endotoxin-free IFN-γ (Sigma-Aldrich Interferon-γ human, cat. #I17001) and TNF-α (Sigma-Aldrich Tumor Necrosis Factor-α human, cat. #H8916) at a final concentration of 10 ng/mL each. PBMCs were incubated for 18 hours at 37 °C and 5% CO_2. Cell-free supernatants were then harvested and immediately analysed for IP-10 production by ELISA (R&D Systems™ Quantikine® ELISA Kit Human CXCL10/IP-10) according to the manufacturer's protocol.

4.7. Statistical analysis

Categorical variables were presented as numbers and percentages, while continuous variables as medians and interquartile ranges (IQR). Mann-Whitney test was used to compare biomarkers of inflammaging between PWH and PWoH, as well as between PWH with detectable serum p24 (p24+) and those with undetectable serum p24 (p24–); the same test was also used to compare total, integrated, and unintegrated HIV DNA between p24+ and p24– PWH. Spearman's correlation test was used to explore correlations between biomarkers of inflammaging in all PWH and correlations between soluble p24 and HIV DNA in p24+ PWH. Linear regression was employed to determine the association between the aforementioned parameters with CD4 T-cell counts and the VACS Index 2.0 in PWH. Factors associated with p24 detectability in PWH were explored by logistic regression; variables with P value <0.2 at univariable analysis were included in the multivariable model. The association between serum p24 [as either binary (detectable/undetectable) or continuous (pg/mL) variable] and biomarkers of inflammaging and CD8+CD38+ cells was determined by univariable and multivariable (adjusting for sex, age, CD4 T-cell count, and ART duration) linear regression analysis. Baseline inflammaging biomarkers and activated CD8 T cells

according to soluble p24 longitudinal patterns were assessed by Kruskall-Wallis test with Dunn's multiple comparisons test or by Mann-Whitney test. Data from *in vitro* independent experiments were expressed as mean and standard error of the mean (SEM), and different stimulation conditions were compared with the unstimulated control using the repeated measures ANOVA with Dunnett's multiple comparisons test.

All statistical analyses were performed by GraphPad Prism 10. P values less than 0.05 were considered statistically significant.

5. Results

5.1. Study population

120 PWH on long-term virologically-suppressive ART and 20 healthy PWoH were enrolled. Demographic, clinical, and HIV-related characteristics of PWH are detailed in **Table 1**. Briefly, median (IQR) age was 54 (47–59) years, 100 (83.3%) were males, and 106 (88.3%) were Caucasian. Median (IQR) CD4 T-cell count was 725 (504–908) cells/μL, with a median (IQR) CD4/CD8 ratio of 0.8 (0.6–1.06). They were on ART for a median (IQR) of 10.25 (6.33–18.5) years, and all of them were virologically suppressed.

5.2. Biomarkers of inflammaging

Firstly, soluble biomarkers of inflammaging were comparatively evaluated in PWH and PWoH to identify inflammaging signatures related to HIV infection. Compared to PWoH, PWH had higher concentrations of plasma IP-10 [median (IQR): 1.908 (1.801–2.048) *versus* 1.792 (1.652–2.009) $\log_{10}$(pg/mL), P=0.0297], TNF-α [median (IQR): 0.8794 (0.7780–0.9366) *versus* 0.7720 (0.7041–0.8156) $\log_{10}$(pg/mL), P=0.0002], IL-17A [median (IQR): 0.4609 (0.1847–0.6881) *versus* 0.3247 (0–0.5090) $\log_{10}$(pg/mL), P=0.0063], IL-8 [median (IQR): 0.7391 (0.5843–0.8800) *versus* 0.5949 (0.4726–0.8172) $\log_{10}$(pg/mL), P=0.0437], sCD14 [median (IQR): 6.433 (6.377–6.503) *versus* 6.357 (6.304–6.449) $\log_{10}$(pg/mL), P=0.0073], sCD163 [median (IQR): 5.676 (5.522–5.829) *versus* 5.587 (5.476–5.695) $\log_{10}$(pg/mL), P=0.0341], TIMP-1 [median (IQR): 1.902 (1.850–1.974) *versus* 1.848 (1.808–1.893) $\log_{10}$(ng/mL), P=0.0130], and GDF-15 [median (IQR): 2.861 (2.707–3.069) *versus* 2.784 (2.690–2.865) $\log_{10}$(pg/mL), P=0.0426] (**Figure 1A,B,E,G,H,I,J,K**). Conversely, no differences were recorded in IL-2, IL-4, IL-6, and ROMO-1 between the two groups (**Figure 1C,D,F,L**).

Activated CD8 T cells (CD8+CD38+ cells) were only measured in PWH. Median (IQR) values were 1.799 (1.544–2.004) $\log_{10}$(cells/μL).

Notably, several positive correlations were found between inflammaging biomarkers in PWH (**Figure S3**, **Supplementary material**). Furthermore, among all of them, only IP-10 was negatively associated with CD4 T-cell count at both univariable and

multivariable (adjusted for sex, age, and ART duration) linear regression analysis (**Table S1**, **Supplementary material**).

5.3. Association of VACS Index 2.0 with biomarkers of inflammaging

Next, the association of inflammaging biomarkers with the estimated mortality risk was evaluated in PWH by univariable linear regression analysis. VACS Index 2.0 was positively associated with IP-10 [β (95% CI): 19.46 (8.433, 30.50), P=0007], TNF-α [β (95% CI): 29.72 (14.50, 44.94), P=0.0002], sCD14 [β (95% CI): 26.41 (2.201, 50.63), P=0.0328], sCD163 [β (95% CI): 15.59 (6.225, 24.95), P=0.0013], TIMP-1 [β (95% CI): 47.13 (27.15, 67.10), P<0.0001], GDF-15 [β (95% CI): 32.97 (25.68, 40.27), P<0.0001], and CD8+CD38+ cells [β (95% CI): 7.859 (0.1479, 15.57), P=0.0458] (**Figure 2A–M**). Yet, by fitting a multivariable linear regression model including all these 7 markers associated with the mortality risk at univariable analysis, only IP-10 and GDF-15 confirmed independently associated with VACS Index 2.0 [β (95% CI): 10.18 (0.2074, 20.15), P=0.0455; β (95% CI): 28.58 (19.51, 37.65), P<0.0001, respectively] (**Figure 2N**).

5.4. Soluble p24

Then, ultra-low level soluble p24 was quantified in serum. A cut-off to discriminate between positive and negative samples was established by analysing serum from PWoH (*n*=20). Based on the results obtained, a value of 0.025 pg/mL (corresponding to 3 standard deviations above the mean signal in plasma from PWoH) was defined as the cut-off to consider an ICD-treated serum sample positive for p24 under the experimental conditions. This value exceeds both the lower limit of detection (LOD=0.0045 pg/mL) and the lower limit of quantification (LOQ=0.0160 pg/mL) proposed for the assay, likely reflecting interference from serum components in protein quantification. By setting this positivity cut-off, 25/120 (20.8%) PWH had detectable soluble p24 [median (range): 0.0516 (0.0264–0.8280) pg/mL) (**Figure 3A**).

When assessing possible factors associated with p24 detectability in PWH by logistic regression, only male sex was associated with p24 detectability at both univariable and multivariable analysis [OR (95% CI): 6.0 (1.147, 110.5), P=0.0309; OR (95% CI): 5.93 (1.101, 110.3), P=0.0361, respectively]. By contrast, age, immunologic

parameters (CD4 T-cell *nadir* ≥350 cells/μL, CD4 T-cell count ≥500 cells/μL, CD4/CD8 ratio ≥0.8), as well as ART duration and regimen were not associated with p24 detectability (**Table 2**).

5.5. Association of soluble p24 with biomarkers of inflammaging

Afterwards, biomarkers of inflammaging were assessed in PWH according to p24 detectability in order to determine whether soluble p24 is associated specific with inflammaging signatures. p24+ PWH showed significantly higher IP-10 levels [median (IQR): 2 (1.869–2.086) *versus* 1.887 (1.779–2.018) $\log_{10}$(pg/mL), P=0.0256] (**Figure 3B**). Conversely, no differences were observed in other soluble biomarkers or in the levels of activated CD8 T cells between p24+ and p24– PWH (**Figure 3C–N**). At multivariable linear regression analysis adjusting for sex, age, CD4 T-cell count, and ART duration, p24 detectability confirmed associated only with higher levels of plasma IP-10 [β (95% CI): 0.1293 (0.0402, 0.2185), P=0.0048] (**Figure 3O**).

Accordingly, when evaluating the association between soluble p24 as continuous variable and plasma IP-10 in p24+ PWH, they proved positively associated to each other at both univariable and multivariable (adjusted for sex, age, CD4 T-cell count, and ART duration) linear regression analysis [β (95% CI): 0.2859 (0.01013, 0.5616), P=0.0428; β (95% CI): 0.3413 (0.07548, 0.6072), P=0.0189, respectively] (**Figure 3P**).

5.6. Longitudinal patterns of soluble p24 and association with baseline biomarkers of inflammaging

Next, the trajectory of soluble p24 was explored in a subset of 30 PWH for whom longitudinal serum samples at 6 months (T1) and 12 months (T2) in addition to baseline (T0) were available. Overall, soluble p24 levels were dynamic over time (**Figure 5A**). In more detail, three different patterns could be identified: 8 PWH were persistently positive for p24 across time points (T0, T1, and T2), 18 PWH were intermittently positive (at one or two time points), whilst 4 PWH were persistently negative at all time points (**Figure 5B–D**).

When assessing baseline inflammaging biomarkers according to soluble p24 longitudinal patterns, a trend towards a decreasing gradient of IP-10 was observed

across persistently positive, intermittently positive, and persistently negative PWH [median (IQR): 2.055 (1.912–2.183) *versus* 1.897 (1.797–2.017) *versus* 1.791 (1.624–2.097) log_{10}(pg/mL), P=0.0739] (**Figure 5E**). In particular, persistently positive PWH had significantly higher baseline IP-10 levels compared to intermittently positive or persistently negative PWH [median (IQR): 2.055 (1.912–2.183) *versus* 1.897 (1.782–2.017) log_{10}(pg/mL), P=0.0270] (**Figure 5F**). No differences in other soluble inflammaging biomarkers or activated CD8 T cells were detected according to the soluble p24 longitudinal patterns (data not shown).

5.7. Cell-associated HIV DNA

Cell-associated HIV DNA was then quantified in a subset of 30 PWH for whom PBMCs at T0 were available in order to explore whether soluble p24 detectability may be associated with larger HIV reservoir (integrated HIV DNA) or residual HIV replication (unintegrated HIV DNA). Total, unintegrated, and integrated HIV DNA did not significantly differ between p24+ and p24– PWH (**Figure 6**). Accordingly, no significant correlations were found between soluble p24 and cell-associated HIV DNA in p24+ PWH (data not shown).

5.8. In vitro confirmatory experiments

To validate the association observed between soluble p24 and IP-10, PBMCs from PWoH were stimulated *in vitro* with varying concentrations of p24. Stimulation with p24 alone did not induce IP-10 secretion in culture supernatants. In contrast, when PBMCs were co-stimulated with IFN-γ and TNF-α, p24 at 10 ng/mL led to a modest but statistically significant increase in IP-10 secretion compared to the unstimulated control [mean (SEM): 2.163 (0.7907) *versus* 2.012 (0.7542) ng/mL, P=0.0478] (**Figure 7**).

6. Discussion

Despite virologically effective ART, PWH continue to experience residual inflammation and immune activation. These processes, typically observed in the elderly and collectively referred to as "inflammaging", drive an increased risk of SNAEs and mortality compared to the general population of similar age. Circulating HIV proteins have been detected in some virologically suppressed PWH, as an expression of the persistence of translation-competent proviruses. In this context, we therefore sought to investigate whether the HIV-related inflammaging state is associated with production of the HIV p24 protein in a cohort of 120 PWH on long-term virologically suppressive ART.

Our results confirmed that PWH feature an inflammaging *milieu* characterised by higher concentrations of plasma IP-10, TNF-α, IL-17A, IL-8, sCD14, sCD163, TIMP-1, and GDF-15 as compared to PWoH (3-7). By contrast, no differences were recorded in IL-2, IL-4, IL-6, and ROMO-1 between the two groups.

Interestingly, consistent with previous reports (87-92), IP-10 was the only biomarker among those measured that showed a negative association with CD4 T-cell count in our cohort, suggesting a strong relationship between this pro-inflammatory chemokine and immune status in PWH.

Notably, when exploring the association of inflammaging biomarkers with the mortality risk as estimated by the VACS Index 2.0, univariable analysis revealed significant positive associations for several biomarkers (IP-10, TNF-α, sCD14, sCD163, TIMP-1, GDF-15, and CD8+CD38+ cells). This finding is in keeping with previous research, that reported a strong association of the VACS Index with several inflammatory markers, such as IL-6 (21, 93), D-dimer (21, 93), sCD14 (21, 94), sCD163 (94), and TNF-α (93). Additionally, a greater inflammation burden as measured as increasing numbers of elevated inflammatory biomarkers above the 75th percentile (particularly 3 or more) has been associated with higher VACS scores in PWH, pointing to a possible additive effect of proinflammatory cytokines in contributing to morbidity and mortality in this population (93). Since the VACS Index is a metric that includes generic measures of multiorgan system injury, its association with markers of inflammation may suggest that chronic inflammation contributes to

end-organ dysfunction and/or that several chronic diseases common among PWH may be proinflammatory.

Remarkably, by fitting a multivariable model including all biomarkers associated with the VACS Index 2.0 at the univariable analysis, only IP-10 and GDF-15 remained independently associated with the VACS Index 2.0 in our study, underscoring their potential predominant role in driving physiological frailty and mortality risk in PWH.

IP-10, also known as CXCL10, is a pro-inflammatory chemokine primarily secreted by innate immune cells, which is involved in the recruitment of innate and adaptive immune cells into sites of inflammation via its CXCR3 receptor (95). IP-10 is strongly implicated in HIV pathogenesis, and has been linked to adverse outcomes in this setting, such as rapid disease progression, cardiovascular diseases, and mortality (89). Elevated circulating IP-10 concentrations have been consistently reported in PWH with rapid HIV disease progression (as defined by faster CD4 T-cell loss) across several studies (91, 92, 96-98). Higher levels of IP-10 – alongside with C reactive protein (CRP), IFN-γ and IL-6 – have been also associated with higher all-cause mortality in a large cohort of people with advanced HIV disease in sub-Saharan Africa (99). Additionally, circulating IP-10 in PWH – besides tumor necrosis factor receptor I (TNFR-I) and II (TNFR-II) – has been linked to increased peri-coronary inflammation as measured by peri-coronary fat attenuation index (FAI) (100), a metric which has been demonstrated to independently predict cardiovascular disease (CVD) risk in the general population (101). This association is further supported by evidences from mouse models and humans indicating a mechanistic role for IP-10 in atherosclerosis and CVD development (102-104).

GDF-15 is a transforming growth factor-β (TGF-β) family member known to regulate several biological processes involved in cell senescence, stress responses, and metabolic regulation (6). It has been proposed as biomarker of aging in PWH (6), and associated with several pathologic conditions in this population, including metabolic disorders (105), hepatic steatosis (106), neurocognitive impairment (107), atherosclerotic coronary plaques (108), cardiovascular dysfunction (109), and all-cause mortality (109).

Several factors have been implicated in the HIV-associated inflammaging state, including the persistence of viral reservoirs despite effective ART, low-level viral

replication, microbial translocation, and coinfections (27). Using an ultra-sensitive assay to quantify soluble p24 in the serum of virologically suppressed PWH following immune complexes dissociation, we found that approximately 21% of participants had detectable p24, albeit at very low levels (<1 pg/mL), despite undetectable plasma HIV RNA. Interestingly, when analysing p24 trajectories in a subset of PWH with available longitudinal samples, soluble p24 levels appeared to be dynamic over a 12-month period, with some PWH being persistently positive, others intermittently positive, and some others persistently negative. This observation suggests that minimal viral protein expression persists even under effective virologic suppression at least in some individuals as an expression of the translationally-competent HIV reservoir.

Previous studies have shown that some PWH on suppressive ART still have detectable HIV proteins (such as p24, gp120, Nef, and Tat) in plasma/serum (40-47), PBMCs (48-52), and tissues (46, 53, 54), as an expression of the persistence of a translationally competent reservoir (30, 50, 56-61). Specifically, p24 has been detected in plasma of some PWH on virologically suppressed ART in earlier studies. By using a signal amplification boosted ELISA on heat-denaturated plasma, Schüpbach *et al.* reported that p24 was detectable in 34% (22/65) of ART-treated PWH after a median of 2 years (range: 6.2–42.8 months) of stably suppressed viremia (HIV RNA <50 copies/mL) (42). The modification of the sample pre-treatment step by the substitution of Triton-X-100–based dissociation buffer with a new SNCR virus disruption buffer, increased the sensitivity of the ELISA, revealing a p24 reactivity in 61.5% (115/187) of PWH exhibiting undetectable HIV RNA below 5 copies/mL for a duration of 6–30 months under ART (43). The mechanisms explaining this enhanced sensitivity remains unclear, but it is plausible that p24 also exists outside viral particles in aggregated forms derived from disrupted virions or lysed virus-producing cells; dispersion of these aggregates into single molecules by the newly developed buffer could have enhanced epitope accessibility and thereby amplified the assay signal (43). The persistence of p24 in PWH with HIV-1 RNA levels <50 copies/mL under ART has then been confirmed by studies employing immuno-PCR or ultrasensitive nanoparticle-based technologies, that uncovered a p24 positivity in 42% (22/52) and 95% (19/20) of virologically suppressed PWH, respectively (110, 111). More recently, the novel digital Simoa technology has been applied to measure p24 in different biological

samples from PWH (40, 112-114). This method represents a major advance in ultrasensitive protein detection, offering up to 1,000-fold greater sensitivity than conventional ELISAs. Passaes *et al*. employed Simoa to measure p24 in the plasma of PWH following acid-mediated immune complexes dissociation, which appeared as the only ICD method compatible with ultrasensitive p24 quantification by this assay. They reported that nearly all individuals with chronic HIV infection had detectable p24 levels prior to ART initiation, which dropped sharply to undetectable following treatment start. Nonetheless, a subset of participants [19/108 (17.6%)] maintained detectable low-level p24 levels 48 weeks after ART initiation, despite most having undetectable viral loads (40). It is noteworthy that reported rates of p24 positivity vary markedly across studies. These discrepancies may reflect differences in sample pre-processing methods, the sensitivity of the assay used for p24 quantification, as well as characteristics of the study populations.

The forces driving the expression of viral proteins in virologically suppressed PWH are poorly characterised. Interestingly, while age, immunologic parameters, and ART duration or regimen were not associated with p24 detectability, male sex emerged as an independent predictor in our analysis. This finding is in accordance with a previous study demonstrating higher levels of cell-associated multiply spliced HIV RNA, as well as a higher ratio of multiply spliced HIV RNA to integrated HIV DNA, in males compared to females, pointing to a greater HIV transcriptional activity in men during suppressive ART (115). These observations also align with prior research reporting fewer HIV RNA-producing cells in ART-naïve women with HIV (116). Lower HIV transcriptional activity in female has also been confirmed *in vitro*, where oestrogens were shown to potently repress HIV transcription in latency models and primary PBMCs from female donors (115, 117). Although these studies focused on cell-associated HIV RNA, our finding on p24 protein is biologically consistent with these data, as viral proteins are produced from viral transcripts. Our results therefore extend prior evidence by demonstrating that sex-based differences in residual HIV expression during suppressive ART are not limited to the transcriptional level, but also translate into detectable protein production.

It remains unclear whether the expression of viral proteins despite virologically suppressive ART reflects a larger HIV reservoir or ongoing residual replication. To

address this, we measured total, integrated, and unintegrated cell-associated HIV DNA in a subset of PWH with available PBMC samples. Integrated HIV DNA is commonly regarded as a marker of the total reservoir size (118), whereas unintegrated HIV DNA forms are considered as an expression of ongoing intracellular viral replication events (119, 120). In keeping with previous studies reporting a lack of association between levels of cell-associated HIV DNA and p24 (40, 42) or gp120 (44) in ART-treated PWH, our analysis showed no significant differences in total, integrated, or unintegrated HIV DNA between p24+ and p24– PWH. Accordingly, no correlation of soluble p24 with HIV DNA was found in p24+ PWH. These findings suggest that soluble p24 positivity under virologic suppression is not explained by an expanded HIV reservoir or by occult residual viral replication. These observations may also indicate that PBMCs are not a major source of serum p24 in PWH on effective ART, that may rather derive from ongoing virus expression in tissue reservoirs not represented by HIV RNA in plasma.

Noteworthy, although highly sensitive single-copy assays may detect residual plasma HIV viraemia in some PWH on suppressive ART (121-123), it is unlikely that the p24 detected in our cohort represents the structural p24 contained in the few viral particles that may be present in plasma or serum. Our sample pre-processing protocol was designed to dissociate immune complexes rather than disrupt viral particles. Since particle-associated p24 is enclosed within the viral core, its detection would require viral lysis, which our method does not achieve. Moreover, previous studies have shown that following ultracentrifugation of plasma from individuals with chronic HIV infection, HIV RNA and reverse transcriptase are completely pelleted, whereas almost all of the p24 remains in the supernatant (124). This observation indicates that most of circulating p24 in PWH is not associated with viral particles but exists in a soluble form, either as free or immune-complexed protein, with a half-life of around 42 days (125).

Persistent protein production during suppressive ART has been linked to systemic inflammation in previous research (44). Antibody responses to viral proteins – a surrogate marker for the presence of viral proteins *in vivo* – correlate with plasma D-dimer levels, while soluble gp120 in plasma has been associated with elevated IL-6. Accordingly, *in vitro* studies further demonstrate that HIV proteins can directly trigger

innate immune activation and pro-inflammatory cytokine and chemokine production (64-72). Remarkably, in line with these observations, we found that soluble p24 is associated with higher IP-10 plasma concentrations, both when analysed as categorical and continuous variable, and independently from other factors such as sex, age, CD4 T-cell count, and ART duration. Furthermore, PWH who were persistently positive for soluble p24 showed the highest baseline IP-10 levels compared to those intermittently positive or persistently negative, further supporting a biologically meaningful relationship between residual HIV protein expression and systemic inflammation. Contrariwise, no associations of p24 cross-sectional or longitudinal status with other soluble inflammaging biomarkers or activated CD8 T-cells were found.

Although no previous studies have described an association between soluble p24 and IP-10 in PWH on ART, it is noteworthy that circulating IP-10 levels have consistently been reported as positively associated with both plasma HIV RNA (88-90, 126-130) and cell-associated HIV DNA (92, 129, 131, 132) across different cohorts, underscoring a strong link between HIV and this pro-inflammatory chemokine. In line with this, *in vitro* studies have demonstrated that HIV strongly induces IP-10 production by innate immune cells, specifically monocytes and myeloid dendritic cells, via TLR7/9-dependent pathways (126). Moreover, IP-10 itself has been shown to enhance HIV entry, replication, and integration in both monocyte-derived macrophages and CD4 T cells (129, 133, 134), further supporting its role as a key mediator at the interface between viral persistence and inflammation.

To validate the association observed between soluble p24 and IP-10, we stimulated PBMCs from PWoH *in vitro* with varying concentrations of p24 and subsequently quantified IP-10 levels in culture supernatants. Since IP-10 expression can be induced by multiple stimuli, and previous studies have shown synergistic effects of IFN-γ and TNF-α on IP-10 production in different cell types (64, 135, 136), p24 stimulation was performed both alone and in combination with IFN-γ and TNF-α to uncover potential synergistic effects. Our results showed that p24 alone did not induce IP-10 secretion by PBMCs; however, in the presence of both IFN-γ and TNF-α, p24 elicited a modest yet significant increase in IP-10 production. These findings not only confirm the association between soluble p24 and IP-10, but also underscore the biological relevance of p24 as a cofactor in IP-10 induction under pro-inflammatory conditions,

suggesting a causal role for this viral protein in contributing to the inflammatory *milieu* in PWH on virologically suppressive ART.

Several limitations should be considered when interpreting our findings. First, the study cohort, although well-characterised, is relatively modest in size, which may limit the generalisability of our results, particularly for specific subgroups such as women or individuals with differing durations of ART. Second, while we included longitudinal p24 measurements in a subset of participants, most analyses are cross-sectional, restricting the ability to draw causal inferences between residual viral protein expression and systemic inflammation; nonetheless, the observed association between p24 and IP-10 is supported by complementary *in vitro* experiments. Third, although we employed an ultrasensitive assay for p24 detection, variability in sample pre-processing may influence detection rates. Fourth, although HIV DNA measurement in PBMCs suggest these cells are unlikely to be the main source of circulating p24, the precise tissue origins of the protein remain uncertain; similarly, plasma biomarkers may not fully reflect processes occurring within tissue reservoirs, which remain unmeasured. Fifth, sex-based differences in p24 expression were observed, but the relatively small number of female participants may limit the robustness of this finding. Finally, the VACS Index 2.0 was used as a surrogate measure of mortality risk, since the predominantly cross-sectional design of the study limited the direct analysis of clinical outcomes; therefore, future studies should confirm these findings by exploring whether soluble p24 detectability in virologically suppressed PWH can predict clinical outcomes, such as SNAEs and/or mortality. Collectively, these limitations highlight the need for larger, longitudinal studies incorporating tissue-level analyses to fully elucidate the mechanisms linking residual viral protein expression, inflammaging, and long-term clinical outcomes in PWH on suppressive ART.

7. Conclusions

In conclusion, our study demonstrates that PWH on long-term virologically suppressive ART continue to experience a state of inflammaging characterised by elevated levels of multiple inflammatory biomarkers, with IP-10 and GDF-15 emerging as independent predictors of multiorgan system injury and mortality risk as estimated by the VACS Index 2.0. Importantly, we provide evidence that soluble HIV p24 protein remains detectable in a subset of virologically suppressed PWH (~21%), and its presence is closely associated with increased IP-10 concentrations, a pro-inflammatory chemokine involved in the recruitment of innate and adaptive immune cells into sites of inflammation. This observation not only extends previous evidence on the translational activity of persistent proviruses, but also provides new insight into how residual viral products might shape the inflammatory landscape of HIV infection despite effective therapy. While the precise sources and mechanisms underlying p24 production remain to be fully elucidated, our data highlight its contribution to IP-10 induction under proinflammatory conditions, suggesting a causal role for this viral protein in maintaining systemic inflammation in PWH on virologically suppressive ART. Further research is warranted to elucidate the pathways driving residual protein production and to determine whether interventions aimed at reducing viral protein expression or blocking its proinflammatory effects could mitigate long-term morbidity and mortality in this population.

8. Tables and figures

Table 1. Demographic, clinical, and HIV-related characteristics of PWH

Characteristics	**PWH (*n*=120)**
Age, years [median (IQR)]	54 (47–59)
Sex [*n* (%)]	
Male	100 (83.3)
Ethnicity [*n* (%)]	
Caucasian	106 (88.3)
African	6 (5)
Latin	5 (4.2)
Asian	3 (2.5)
Epidemiology [*n* (%)]	
MSM	59 (49.2)
MSW/WSM	37 (30.8)
IDU	22 (18.3)
Unknown	2 (1.7)
Comorbidities [*n* (%)]	
None	66 (55)
Cardiovascular disease	32 (26.7)
Chronic kidney disease	15 (12.5)
Liver disease	17 (14.2)
COPD/asthma	11 (9.2)
Neurologic disease	13 (10.8)
Gastrointestinal disease	10 (8.3)
Diabetes	19 (15.8)
Autoimmune diseases	18 (15)
Previous leukemia/lymphoma	13 (10.8)
Previous solid tumor	12 (10)
Viro-immunologic parameters	
CD4 T-cell *nadir*, cells/µL [median (IQR)]	226 (55–372)
CD4 T-cell count, cells/µL [median (IQR)]	725 (504–908)
CD4 T-cell percentage, % [median (IQR)]	32 (25–38)
CD8 T-cell count, cells/µL [median (IQR)]	893 (667–1162)
CD8 T-cell percentage, % [median (IQR)]	40 (34–45)
CD4/CD8 ratio [median (IQR)]	0.8 (0.6–1.06)
CD4 T-cell *nadir* ≥350 cells/µL [*n* (%)]	32 (26.7)
CD4 T-cell count ≥500 cells/µL [*n* (%)]	90 (75)
CD4/CD8 ratio ≥0.8 [*n* (%)]	60 (50)
HIV-RNA <20 copies/mL [*n* (%)]	120 (100)
Previous AIDS diagnosis [*n* (%)]	80 (66.7)
Time from HIV diagnosis, years [median (IQR)]	11.25 (7.33–25.25)
Current ART regimen [*n* (%)]	
INSTI-based triple	55 (45.8)
INSTI-based dual	27 (22.5)
PI-based	4 (3.3)
NNRTI-based triple	34 (28.3)

Duration of ART, years [median (IQR)]	10.25 (6.33–18.5)
Legend: *PWH*, people with HIV; *IQR*, interquartile range; *MSM*, men who have sex with men; *MSW*, men who have sex with women; *WSM*, women who have sex with men; *IDU*, injective drug user; *COPD*, chronic obstructive pulmonary disease; *ART*, antiretroviral therapy; *INSTI*, integrase strand transfer inhibitor; *PI*, protease inhibitor; *NNRTI*, non-nucleoside reverse transcriptase inhibitors	

Table 2. Logistic regression analysis exploring possible factors associated with p24 detectability in PWH (variables with P value <0.2 at univariable analysis included in the multivariable model)

Variables	**Univariable analysis**			**Multivariable analysis**		
	OR	**95% CI**	**P value**	**OR**	**95% CI**	**P value**
Age (years)	1.002	0.9591, 1.047	0.9336			
Male sex	6.0	1.147, 110.5	**0.0309**	5.930	1.101, 110.3	**0.0361**
CD4 T-cell *nadir* ≥350 cells/μL	2.212	0.8552, 5.598	0.1000	1.505	0.5455, 4.070	0.4239
CD4 T-cell count ≥500 cells/μL	2.763	0.8628, 12.36	0.0906	2.240	0.6288, 10.61	0.2241
CD4/CD8 ratio ≥0.8	1.975	0.8083, 5.084	0.1366	1.605	0.6199, 4.325	0.3313
Duration of ART (months)	0.9973	0.9922, 1.002	0.2619			
INSTI-based triple ART	1.367	0.5635, 3.343	0.4874			
INSTI-based dual ART	1.882	0.6820, 4.936	0.2147			
Legend: *OR*, odds ratio; *95% CI*, 95% confidence interval; *INSTI*, integrase strand transfer inhibitor						

Figure 1. Soluble biomarkers of inflammaging in PWH. Plasma concentrations of IP-10 (**A**), TNF-α (**B**), IL-2 (**C**), IL-4 (**D**), IL-17A (**E**), IL-6 (**F**), IL-8 (**G**), sCD14 (**H**), sCD163 (**I**), TIMP-1 (**J**), GDF-15 (**K**), ROMO-1 (**L**) in PWH (*n*=120) and PWoH (*n*=20). *Blue circles*: individual values (PWH); *yellow circles*: individual values (PWoH); *black bars*: median values; *blue/yellow boxes*: interquartile ranges; *statistical analysis:* Mann-Whitney test (P values reported above the line connecting the two groups; P values <0.05 shown in red).

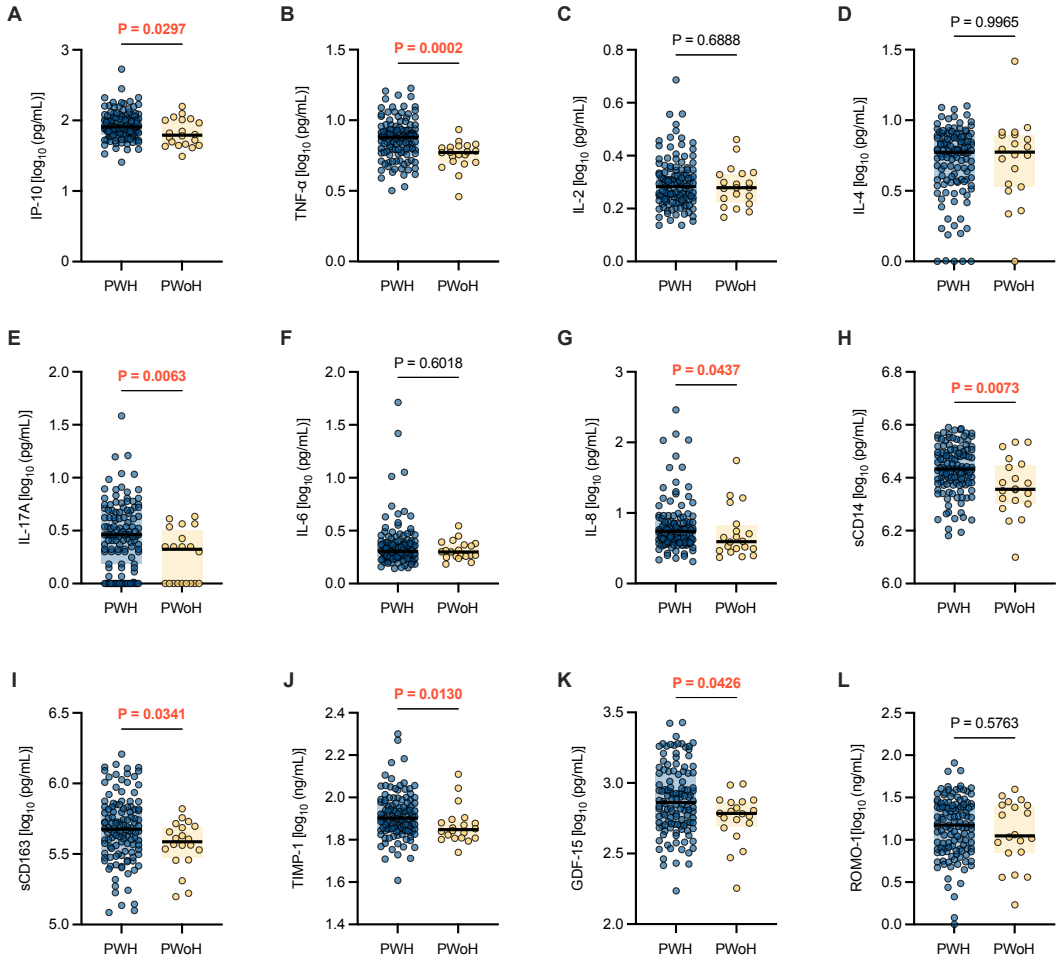

Figure 2. Association of biomarkers of inflammaging with the VACS Index 2.0. (**A–M**) Univariable linear regression analysis exploring the association of biomarkers of inflammaging with the mortality risk as estimated by the VACS Index 2.0 (P values <0.05 shown in red) in PWH (*n*=120). *Blue circles*: individual values; *black line*: fitted line; *β*: β coefficient; *95% CI*: 95% confidence interval. (**N**) Forest plot showing the results of the multivariable linear regression analysing biomarkers independently associated with the VACS Index 2.0 (variables with P value <0.05 at the univariable linear regression and shown in the forest plot included in the multivariable model; P values <0.05 shown in red). *Grey circles*: β coefficients; *error bars*: 95% confidence intervals.

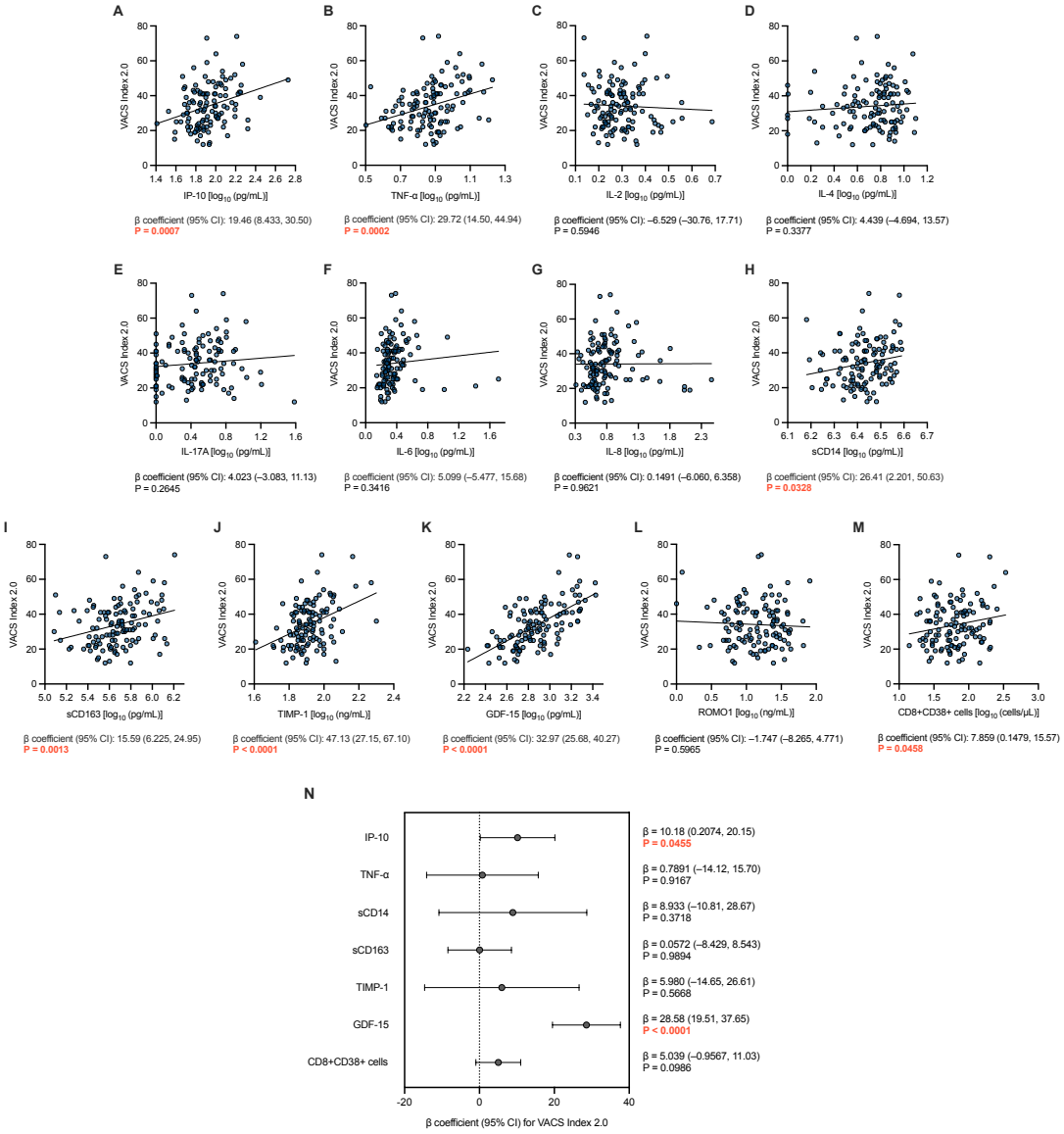

Figure 3. Soluble p24 and biomarkers of inflammaging according to p24 detectability. (**A**) Soluble p24 in PWoH (*n*=20) and PWH (*n*=120). *Dashed line*: positivity cut-off [0.025 pg/mL (calculated as the mean + 3SD of values in PWoH)]; *teal circles*: individual values above the positivity cut-off; *grey circles*: individual values below the positivity cut-off. (**B–N**) Biomarkers of inflammaging in PWH (*n*=120) with detectable or undetectable soluble p24 (p24+ and p24–, respectively). *Dashed lines*: median values in PWoH; *teal circles*: individual values (p24+ PWH); *grey circles*: individual values (p24– PWH); *black bars*: median values; *teal/grey boxes*: interquartile ranges; *statistical analysis:* Mann-Whitney test (P values reported above the line connecting the two groups; P values <0.05 shown in red).

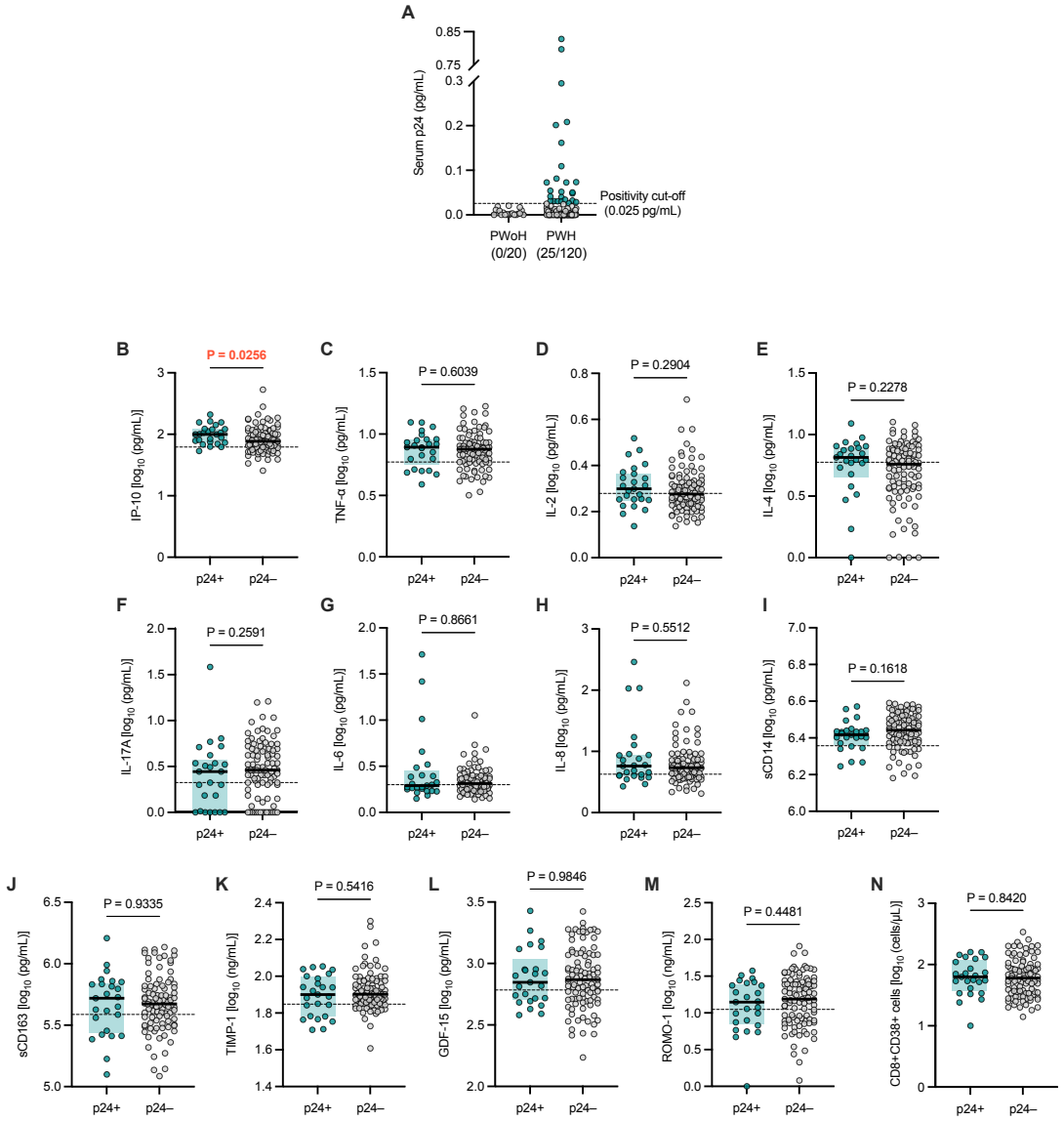

Figure 4. Association of soluble p24 with biomarkers of inflammaging. (**A**) Forest plot showing the results of the multivariable linear regression analysis exploring biomarkers independently associated with the soluble p24 positivity in PWH adjusted for sex, age, CD4 T-cell count, and ART duration (P values <0.05 shown in red). *Grey circles*: β coefficients; *error bars*: 95% confidence intervals. (**B**) Univariable and multivariable (adjusted for sex, age, CD4 T-cell count, and ART duration) linear regression analysing the association between soluble p24 and IP-10 in PWH with detectable p24. *Teal circles*: individual values; *black line*: fitted line; *β*: β coefficient; *95% CI*: 95% confidence interval.

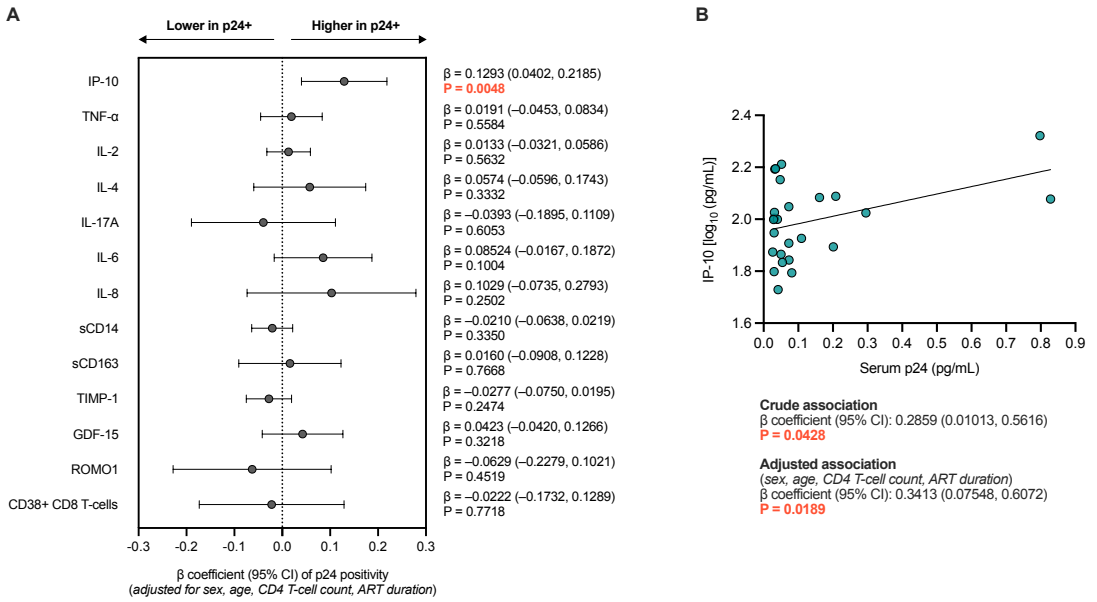

Figure 5. Longitudinal patterns of soluble p24 and association with inflammation. (**A–D**) Soluble p24 in a subset of PWH with available longitudinal samples (*n*=30) at baseline (T0), 6 months (T1), and 12 months (T2). *Dashed line*: positivity cut-off [0.025 pg/mL (calculated as the mean + 3SD of values in PWoH)]; *teal circles*: individual values above the positivity cut-off; *grey circles*: individual values below the positivity cut-off. (**E**) Plasma concentrations of IP-10 at T0 in persistently positive *versus* intermittently positive *versus* persistently negative PWH. *Circles*: individual values; *boxes*: interquartile ranges; *statistical analysis*: Kruskall-Wallis test with Dunn's multiple comparisons test (P values reported above the line connecting the groups). (**F**) Plasma concentrations of IP-10 at T0 in persistently positive *versus* intermittently positive or persistently negative PWH. *Circles*: individual values; *boxes*: interquartile ranges; *statistical analysis*: Mann-Whitney test (P values reported above the line connecting the two groups; P values <0.05 shown in red).

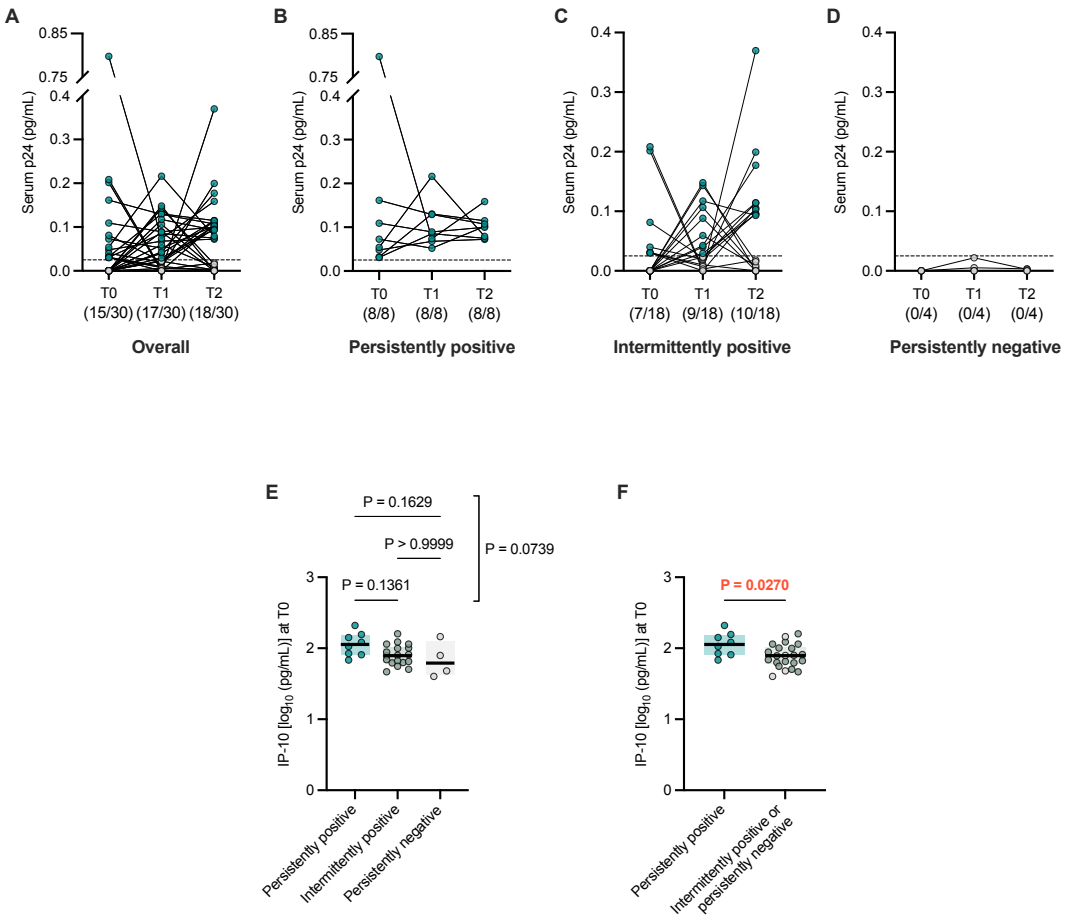

Figure 6. Cell-associated HIV DNA in PWH. Total (**A**), unintegrated (**B**), and integrated (**C**) HIV DNA in a subset of PWH with detectable soluble p24 (p24+, *n*=7) and with undetectable soluble p24 (p24–, *n*=23). *Teal circles*: individual values (p24+ PWH); *grey circles*: individual values (p24– PWH); *black bars*: median values; *teal/grey boxes*: interquartile ranges; *statistical analysis:* Mann-Whitney test (P values reported above the line connecting the two groups).

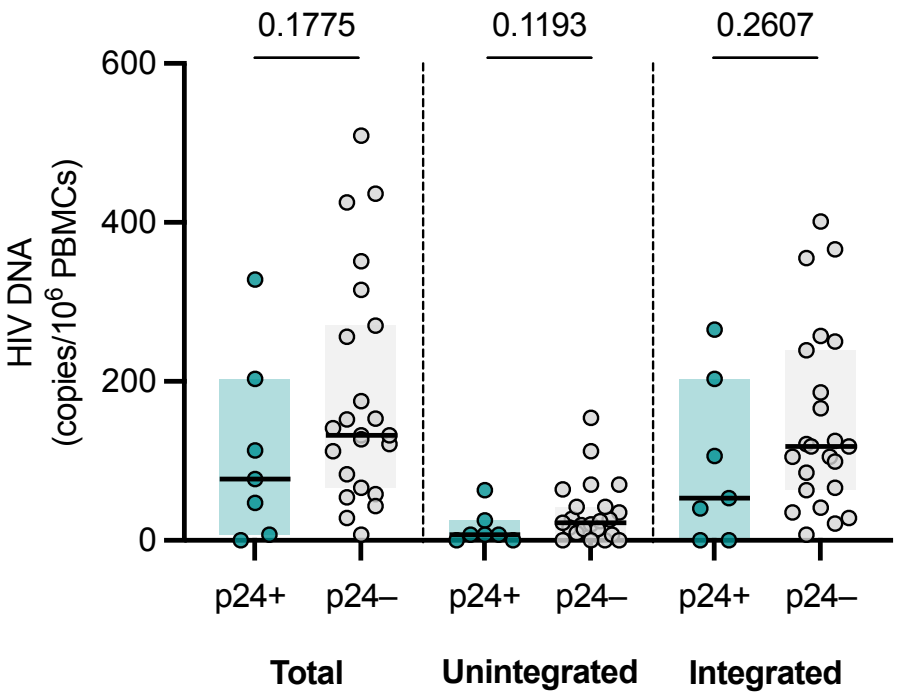

Figure 7. Soluble p24 can induce IP-10 secretion by PBMCs in the presence of IFN-γ and TNF-α *in vitro*. PBMCs from PWoH (*n*=6) were stimulated in duplicate for 18 hours with endotoxin-free recombinant p24 at four different concentrations (100 ng/mL, 10 ng/mL, 1 ng/mL, 0.1 ng/mL) either alone or in the presence of both IFN-γ and TNF-α at a concentration of 10 ng/mL each; IP-10 was then quantified by ELISA in cell-free supernatants. *Yellow circles*: mean values; *error bars*: standard error of the mean (SEM); *statistical analysis*: repeated measures ANOVA (P values reported above the lines connecting each p24 concentration with the unstimulated control; P values <0.05 shown in red).

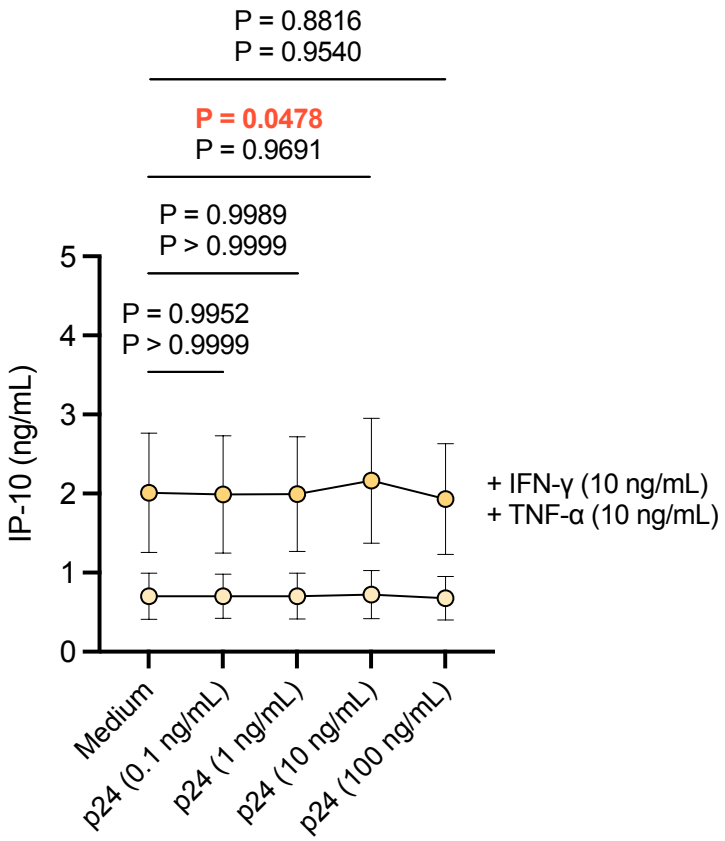

9. Supplementary material

Table S1. Linear regression analysis exploring biomarkers of inflammaging associated with the CD4 T-cell count (cells/µL) in PWH (*n*=120)

Variables	Univariable analysis			Multivariable analysis*		
	β	**95% CI**	**P value**	**β**	**95% CI**	**P value**
IP-10 [log_{10}(pg/mL)]	–309.4	–561.6, –48.21	**0.0203**	–325.4	–588.6, –62.22	**0.0158**
TNF-α [log_{10}(pg/mL)]	–167.3	–537.5, 202.9	0.3725	–202.3	–593.4, 188.8	0.3077
IL-2 [log_{10}(pg/mL)]	160.1	–392.4, 712.6	0.5672	162.5	–394.8, 719.9	0.5646
IL-4 [log_{10}(pg/mL)]	52.17	–155.6, 260	0.6199	53.06	–162.2, 268.3	0.6263
IL-17A [log_{10}(pg/mL)]	–158.5	–317.9, 0.8207	0.0512	–158	–321, 5.077	0.0574
IL-6 [log_{10}(pg/mL)]	163.1	–76.04, 402.1	0.1794	172.1	–69.36, 413.5	0.1607
IL-8 [log_{10}(pg/mL)]	96.81	–42.96, 236.6	0.1727	94.98	–45.76, 235.7	0.1839
sCD14 [log_{10}(pg/mL)]	119.9	–442.2, 682	0.6733	31.31	–564.4, 627	0.9172
sCD163 [log_{10}(pg/mL)]	34.26	–187.8, 256.3	0.7605	–3.609	–242.4, 235.2	0.9762
TIMP-1 [log_{10}(pg/mL)]	119.1	–374.7, 612.9	0.6337	122	–410.5, 654.4	0.6508
GDF-15 [log_{10}(pg/mL)]	–55.18	–269.8, 159.5	0.6116	–143.1	–441.1, 155	0.3436
ROMO1 [log_{10}(ng/mL)]	15.62	–133.1, 164.3	0.8356	7.66	–146.1, 161.4	0.9215
CD8+CD38+ cells [log_{10}(cells/µL)]	84.45	–91.29, 260.2	0.3431	81.29	–95.89, 258.5	0.3652
Legend: *β*, β coefficient; *95% CI*, 95% confidence interval * Adjusted for sex, age, and ART duration						

Figure S1. Gating strategy for the identification of activated CD8 T cells (CD8+CD38+ cells) in a representative sample (fresh whole blood). See "Methods" for details on the methodology.

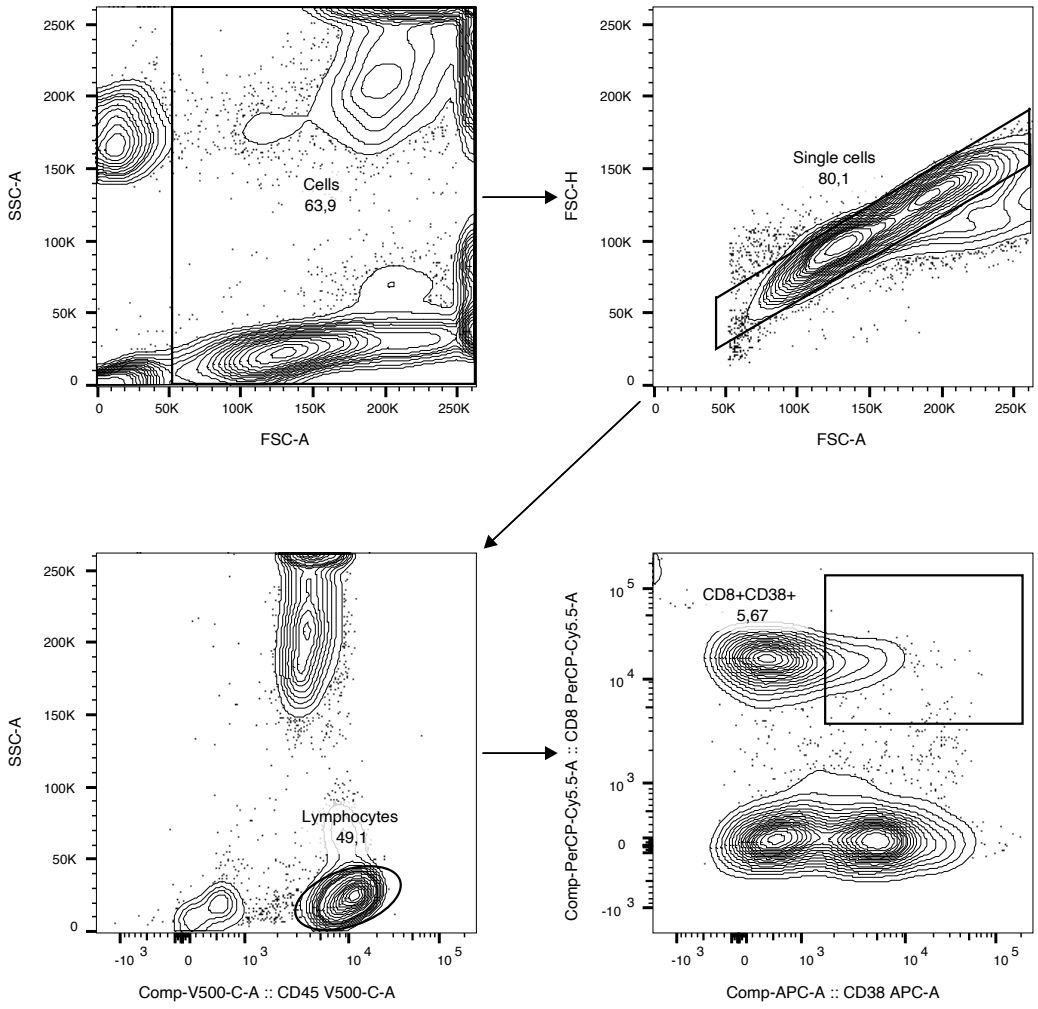

Figure S2. Effect of acid pre-treatment on soluble p24 quantification in serum. Exploratory experiments in PWH on virologically suppressive antiretroviral therapy (*n*=14) showed that acid pre-treatment of serum to induce the immune complexes dissociation (ICD) is able to significantly increase both the serum p24 levels and the detectability rate above the limit of detection (LOD) specified in the assay data sheet (0.0045 pg/mL) as compared to the non-treated (NT) serum samples. *Statistical test*: Wilcoxon test. See "Methods" for details on the methodology.

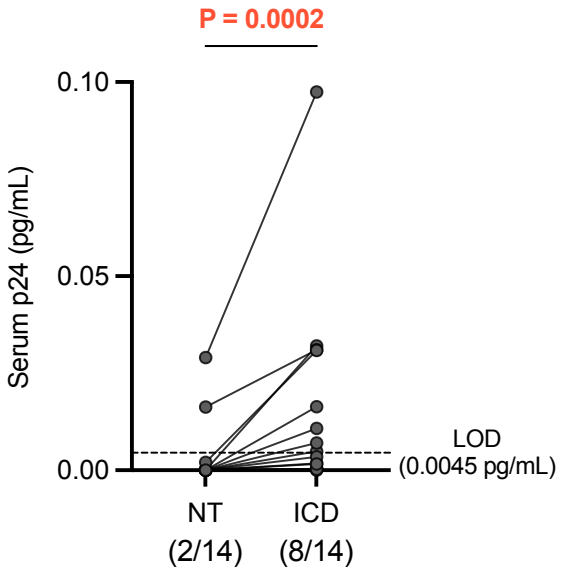

Figure S3. Correlations between biomarkers of inflammaging. Heatmap showing correlations between biomarkers of inflammaging in PWH (*n*=120). *Red cells*: positive correlations (r>0); *blue cells*: negative correlations (r<0); *statistical analysis*: Spearman's correlation test (r values are reported within the cells; correlations with P values <0.05 are indicated with an asterisk).

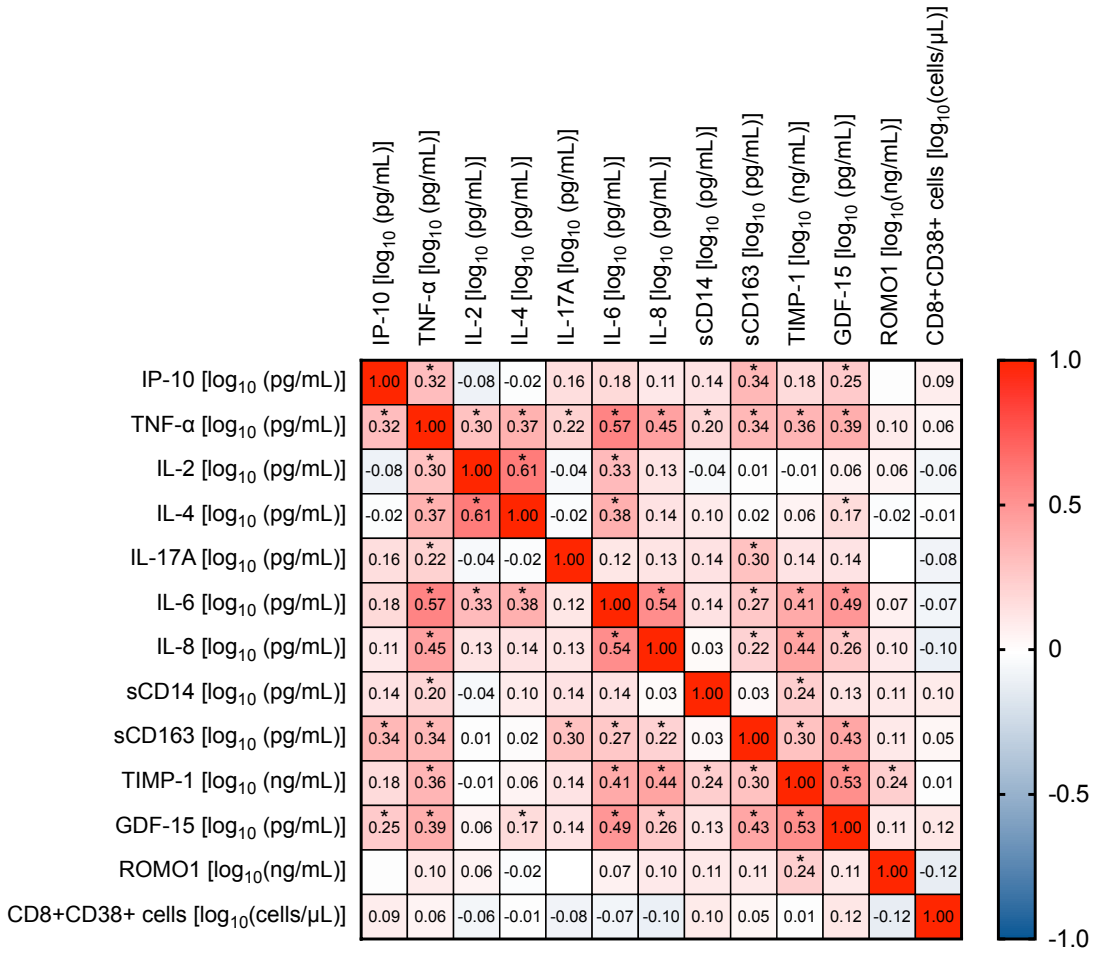

10. References

1. Palella FJ, Delaney KM, Moorman AC, Loveless MO, Fuhrer J, Satten GA, et al. Declining morbidity and mortality among patients with advanced human immunodeficiency virus infection. HIV Outpatient Study Investigators. N Engl J Med. 1998;338(13):853-60.
2. O'Brien WA, Hartigan PM, Daar ES, Simberkoff MS, Hamilton JD. Changes in plasma HIV RNA levels and CD4+ lymphocyte counts predict both response to antiretroviral therapy and therapeutic failure. VA Cooperative Study Group on AIDS. Ann Intern Med. 1997;126(12):939-45.
3. Sieg SF, Shive CL, Panigrahi S, Freeman ML. Probing the Interface of HIV and Inflammaging. Curr HIV/AIDS Rep. 2021;18(3):198-210.
4. Hunt PW. HIV and inflammation: mechanisms and consequences. Curr HIV/AIDS Rep. 2012;9(2):139-47.
5. Sheets K, Baker JV. HIV and Inflamm-Aging: How Do We Reach the Summit of Healthy Aging? Top Antivir Med. 2024;32(5):589-96.
6. Wang L, Zhao J, Schank M, Hill AC, Banik P, Zhang Y, et al. Circulating GDF-15: a biomarker for metabolic dysregulation and aging in people living with HIV. Front Aging. 2024;5:1414866.
7. Agarwal N, Ramirez Bustamante CE, Wu H, Armamento-Villareal R, Lake JE, Balasubramanyam A, et al. Heightened levels of plasma growth differentiation factor 15 in men living with HIV. Physiol Rep. 2022;10(9):e15293.
8. Hileman CO, Funderburg NT. Inflammation, Immune Activation, and Antiretroviral Therapy in HIV. Curr HIV/AIDS Rep. 2017;14(3):93-100.
9. Kuller LH, Tracy R, Belloso W, De Wit S, Drummond F, Lane HC, et al. Inflammatory and coagulation biomarkers and mortality in patients with HIV infection. PLoS Med. 2008;5(10):e203.
10. Baker JV, Sharma S, Grund B, Rupert A, Metcalf JA, Schechter M, et al. Systemic Inflammation, Coagulation, and Clinical Risk in the START Trial. Open Forum Infect Dis. 2017;4(4):ofx262.

11. Wada NI, Bream JH, Martínez-Maza O, Macatangay B, Galvin SR, Margolick JB, et al. Inflammatory Biomarkers and Mortality Risk Among HIV-Suppressed Men: A Multisite Prospective Cohort Study. Clin Infect Dis. 2016;63(7):984-90.
12. Tenorio AR, Zheng Y, Bosch RJ, Krishnan S, Rodriguez B, Hunt PW, et al. Soluble markers of inflammation and coagulation but not T-cell activation predict non-AIDS-defining morbid events during suppressive antiretroviral treatment. J Infect Dis. 2014;210(8):1248-59.
13. Marcus JL, Leyden WA, Alexeeff SE, Anderson AN, Hechter RC, Hu H, et al. Comparison of Overall and Comorbidity-Free Life Expectancy Between Insured Adults With and Without HIV Infection, 2000-2016. JAMA Netw Open. 2020;3(6):e207954.
14. Hart BB, Nordell AD, Okulicz JF, Palfreeman A, Horban A, Kedem E, et al. Inflammation-Related Morbidity and Mortality Among HIV-Positive Adults: How Extensive Is It? J Acquir Immune Defic Syndr. 2018;77(1):1-7.
15. Hsu DC, Sereti I, Ananworanich J. Serious Non-AIDS events: Immunopathogenesis and interventional strategies. AIDS Res Ther. 2013;10(1):29.
16. Hsu DC, Sereti I. Serious Non-AIDS Events: Therapeutic Targets of Immune Activation and Chronic Inflammation in HIV Infection. Drugs. 2016;76(5):533-49.
17. Lundgren JD, Babiker AG, Gordin F, Emery S, Grund B, Sharma S, et al. Initiation of Antiretroviral Therapy in Early Asymptomatic HIV Infection. N Engl J Med. 2015;373(9):795-807.
18. Grinspoon SK, Fitch KV, Zanni MV, Fichtenbaum CJ, Umbleja T, Aberg JA, et al. Pitavastatin to Prevent Cardiovascular Disease in HIV Infection. N Engl J Med. 2023;389(8):687-99.
19. Justice AC, Tate JP. Strengths and Limitations of the Veterans Aging Cohort Study Index as a Measure of Physiologic Frailty. AIDS Res Hum Retroviruses. 2019;35(11-12):1023-33.
20. Tate JP, Justice AC, Hughes MD, Bonnet F, Reiss P, Mocroft A, et al. An internationally generalizable risk index for mortality after one year of antiretroviral therapy. AIDS. 2013;27(4):563-72.
21. Justice AC, Freiberg MS, Tracy R, Kuller L, Tate JP, Goetz MB, et al. Does an index composed of clinical data reflect effects of inflammation, coagulation, and

monocyte activation on mortality among those aging with HIV? Clin Infect Dis. 2012;54(7):984-94.

22. Tate JP, Sterne JAC, Justice AC, (ART-CC) VACSVatATCC. Albumin, white blood cell count, and body mass index improve discrimination of mortality in HIV-positive individuals. AIDS. 2019;33(5):903-12.

23. McGinnis KA, Justice AC, Moore RD, Silverberg MJ, Althoff KN, Karris M, et al. Discrimination and Calibration of the Veterans Aging Cohort Study Index 2.0 for Predicting Mortality Among People With Human Immunodeficiency Virus in North America. Clin Infect Dis. 2022;75(2):297-304.

24. Ambia J, Ingle SM, McGinnis K, Pantazis N, Silverberg MJ, Wittkop L, et al. Discrimination of the Veterans Aging Cohort Study Index 2.0 for Predicting Cause-specific Mortality Among Persons With HIV in Europe and North America. Open Forum Infect Dis. 2024;11(7):ofae333.

25. Qian Y, Moore RD, Coburn SB, Davy-Mendez T, Akgün KM, McGinnis KA, et al. Association of the VACS Index With Hospitalization Among People With HIV in the NA-ACCORD. J Acquir Immune Defic Syndr. 2022;89(1):9-18.

26. Hernández-Favela CG, Hernández-Ruiz VA, Bello-Chavolla OY, Crabtree-Ramírez B, Sierra-Madero J, Amieva H, et al. Higher Veterans Aging Cohort Study 2.0 Index Score Predicts Functional Decline Among Older Adults Living with HIV. AIDS Res Hum Retroviruses. 2021;37(11):878-83.

27. Deeks SG. HIV infection, inflammation, immunosenescence, and aging. Annu Rev Med. 2011;62:141-55.

28. Siliciano JM, Siliciano RF. The Remarkable Stability of the Latent Reservoir for HIV-1 in Resting Memory CD4+ T Cells. J Infect Dis. 2015;212(9):1345-7.

29. Veenhuis RT, Abreu CM, Costa PAG, Ferreira EA, Ratliff J, Pohlenz L, et al. Monocyte-derived macrophages contain persistent latent HIV reservoirs. Nat Microbiol. 2023;8(5):833-44.

30. Imamichi H, Smith M, Adelsberger JW, Izumi T, Scrimieri F, Sherman BT, et al. Defective HIV-1 proviruses produce viral proteins. Proc Natl Acad Sci U S A. 2020;117(7):3704-10.

31. Fletcher CV, Staskus K, Wietgrefe SW, Rothenberger M, Reilly C, Chipman JG, et al. Persistent HIV-1 replication is associated with lower antiretroviral drug concentrations in lymphatic tissues. Proc Natl Acad Sci U S A. 2014;111(6):2307-12.
32. Estes JD, Kityo C, Ssali F, Swainson L, Makamdop KN, Del Prete GQ, et al. Defining total-body AIDS-virus burden with implications for curative strategies. Nat Med. 2017;23(11):1271-6.
33. Martinez-Picado J, Deeks SG. Persistent HIV-1 replication during antiretroviral therapy. Curr Opin HIV AIDS. 2016;11(4):417-23.
34. Brenchley JM, Price DA, Schacker TW, Asher TE, Silvestri G, Rao S, et al. Microbial translocation is a cause of systemic immune activation in chronic HIV infection. Nat Med. 2006;12(12):1365-71.
35. Marchetti G, Tincati C, Silvestri G. Microbial translocation in the pathogenesis of HIV infection and AIDS. Clin Microbiol Rev. 2013;26(1):2-18.
36. Kovacs A, Al-Harthi L, Christensen S, Mack W, Cohen M, Landay A. CD8(+) T cell activation in women coinfected with human immunodeficiency virus type 1 and hepatitis C virus. J Infect Dis. 2008;197(10):1402-7.
37. Gonzalez VD, Falconer K, Blom KG, Reichard O, Mørn B, Laursen AL, et al. High levels of chronic immune activation in the T-cell compartments of patients coinfected with hepatitis C virus and human immunodeficiency virus type 1 and on highly active antiretroviral therapy are reverted by alpha interferon and ribavirin treatment. J Virol. 2009;83(21):11407-11.
38. Sullivan ZA, Wong EB, Ndung'u T, Kasprowicz VO, Bishai WR. Latent and Active Tuberculosis Infection Increase Immune Activation in Individuals Co-Infected with HIV. EBioMedicine. 2015;2(4):334-40.
39. Wittkop L, Bitard J, Lazaro E, Neau D, Bonnet F, Mercie P, et al. Effect of cytomegalovirus-induced immune response, self antigen-induced immune response, and microbial translocation on chronic immune activation in successfully treated HIV type 1-infected patients: the ANRS CO3 Aquitaine Cohort. J Infect Dis. 2013;207(4):622-7.
40. Passaes C, Delagreverie HM, Avettand-Fenoel V, David A, Monceaux V, Essat A, et al. Ultrasensitive Detection of p24 in Plasma Samples from People with Primary and Chronic HIV-1 Infection. J Virol. 2021;95(14):e0001621.

41. Schüpbach J, Böni J, Bisset LR, Tomasik Z, Fischer M, Günthard HF, et al. HIV-1 p24 antigen is a significant inverse correlate of CD4 T-cell change in patients with suppressed viremia under long-term antiretroviral therapy. J Acquir Immune Defic Syndr. 2003;33(3):292-9.

42. Schüpbach J, Günthard H, Joos B, Fischer M, Böni J, Tomasik Z, et al. HIV-1 p24 may persist during long-term highly active antiretroviral therapy, increases little during short treatment breaks, and its rebound after treatment stop correlates with CD4(+) T cell loss. J Acquir Immune Defic Syndr. 2005;40(3):250-6.

43. Schüpbach J, Tomasik Z, Knuchel M, Opravil M, Günthard HF, Nadal D, et al. Optimized virus disruption improves detection of HIV-1 p24 in particles and uncovers a p24 reactivity in patients with undetectable HIV-1 RNA under long-term HAART. J Med Virol. 2006;78(8):1003-10.

44. Benlarbi M, Richard J, Bourassa C, Tolbert WD, Chartrand-Lefebvre C, Gendron-Lepage G, et al. Plasma Human Immunodeficiency Virus 1 Soluble Glycoprotein 120 Association With Correlates of Immune Dysfunction and Inflammation in Antiretroviral Therapy-Treated Individuals With Undetectable Viremia. J Infect Dis. 2024;229(3):763-74.

45. Ferdin J, Goričar K, Dolžan V, Plemenitaš A, Martin JN, Peterlin BM, et al. Viral protein Nef is detected in plasma of half of HIV-infected adults with undetectable plasma HIV RNA. PLoS One. 2018;13(1):e0191613.

46. Gupta MK, Kaminski R, Mullen B, Gordon J, Burdo TH, Cheung JY, et al. HIV-1 Nef-induced cardiotoxicity through dysregulation of autophagy. Sci Rep. 2017;7(1):8572.

47. Shmakova A, Tsimailo I, Kozhevnikova Y, Gérard L, Boutboul D, Oksenhendler E, et al. HIV-1 Tat is present in the serum of people living with HIV-1 despite viral suppression. Int J Infect Dis. 2024;142:106994.

48. Wang T, Green LA, Gupta SK, Amet T, Byrd DJ, Yu Q, et al. Intracellular Nef detected in peripheral blood mononuclear cells from HIV patients. AIDS Res Hum Retroviruses. 2015;31(2):217-20.

49. Pardons M, Baxter AE, Massanella M, Pagliuzza A, Fromentin R, Dufour C, et al. Single-cell characterization and quantification of translation-competent viral reservoirs in treated and untreated HIV infection. PLoS Pathog. 2019;15(2):e1007619.

50. Baxter AE, Niessl J, Fromentin R, Richard J, Porichis F, Charlebois R, et al. Single-Cell Characterization of Viral Translation-Competent Reservoirs in HIV-Infected Individuals. Cell Host Microbe. 2016;20(3):368-80.
51. Dubé M, Tastet O, Dufour C, Sannier G, Brassard N, Delgado GG, et al. Spontaneous HIV expression during suppressive ART is associated with the magnitude and function of HIV-specific CD4. Cell Host Microbe. 2023;31(9):1507-22.e5.
52. DeMaster LK, Liu X, VanBelzen DJ, Trinité B, Zheng L, Agosto LM, et al. A Subset of CD4/CD8 Double-Negative T Cells Expresses HIV Proteins in Patients on Antiretroviral Therapy. J Virol. 2015;90(5):2165-79.
53. Wu G, Zuck P, Goh SL, Milush JM, Vohra P, Wong JK, et al. Gag p24 Is a Marker of Human Immunodeficiency Virus Expression in Tissues and Correlates With Immune Response. J Infect Dis. 2021;224(9):1593-8.
54. Santosuosso M, Righi E, Lindstrom V, Leblanc PR, Poznansky MC. HIV-1 envelope protein gp120 is present at high concentrations in secondary lymphoid organs of individuals with chronic HIV-1 infection. J Infect Dis. 2009;200(7):1050-3.
55. Cole B, Lambrechts L, Gantner P, Noppe Y, Bonine N, Witkowski W, et al. In-depth single-cell analysis of translation-competent HIV-1 reservoirs identifies cellular sources of plasma viremia. Nat Commun. 2021;12(1):3727.
56. Kuniholm J, Armstrong E, Bernabe B, Coote C, Berenson A, Patalano SD, et al. Intragenic proviral elements support transcription of defective HIV-1 proviruses. PLoS Pathog. 2021;17(12):e1009982.
57. Pollack RA, Jones RB, Pertea M, Bruner KM, Martin AR, Thomas AS, et al. Defective HIV-1 Proviruses Are Expressed and Can Be Recognized by Cytotoxic T Lymphocytes, which Shape the Proviral Landscape. Cell Host Microbe. 2017;21(4):494-506.e4.
58. Singh K, Natarajan V, Dewar R, Rupert A, Badralmaa Y, Zhai T, et al. Long-term persistence of transcriptionally active 'defective' HIV-1 proviruses: implications for persistent immune activation during antiretroviral therapy. AIDS. 2023;37(14):2119-30.
59. Olson A, Coote C, Snyder-Cappione JE, Lin N, Sagar M. HIV-1 Transcription but Not Intact Provirus Levels are Associated With Systemic Inflammation. J Infect Dis. 2021;223(11):1934-42.

60. Scrimieri F, Bastian E, Smith M, Rehm CA, Morse C, Kuruppu J, et al. Transcriptionally Active Defective HIV-1 Proviruses and Their Association With Immunological Nonresponse to Antiretroviral Therapy. J Infect Dis. 2024;229(6):1786-90.
61. Baxter AE, O'Doherty U, Kaufmann DE. Beyond the replication-competent HIV reservoir: transcription and translation-competent reservoirs. Retrovirology. 2018;15(1):18.
62. Akiyama H, Miller CM, Ettinger CR, Belkina AC, Snyder-Cappione JE, Gummuluru S. HIV-1 intron-containing RNA expression induces innate immune activation and T cell dysfunction. Nat Commun. 2018;9(1):3450.
63. McCauley SM, Kim K, Nowosielska A, Dauphin A, Yurkovetskiy L, Diehl WE, et al. Intron-containing RNA from the HIV-1 provirus activates type I interferon and inflammatory cytokines. Nat Commun. 2018;9(1):5305.
64. Williams R, Yao H, Dhillon NK, Buch SJ. HIV-1 Tat co-operates with IFN-gamma and TNF-alpha to increase CXCL10 in human astrocytes. PLoS One. 2009;4(5):e5709.
65. Levast B, Barblu L, Coutu M, Prévost J, Brassard N, Peres A, et al. HIV-1 gp120 envelope glycoprotein determinants for cytokine burst in human monocytes. PLoS One. 2017;12(3):e0174550.
66. Del Cornò M, Cappon A, Donninelli G, Varano B, Marra F, Gessani S. HIV-1 gp120 signaling through TLR4 modulates innate immune activation in human macrophages and the biology of hepatic stellate cells. J Leukoc Biol. 2016;100(3):599-606.
67. Nazli A, Kafka JK, Ferreira VH, Anipindi V, Mueller K, Osborne BJ, et al. HIV-1 gp120 induces TLR2- and TLR4-mediated innate immune activation in human female genital epithelium. J Immunol. 2013;191(8):4246-58.
68. Planès R, Serrero M, Leghmari K, BenMohamed L, Bahraoui E. HIV-1 Envelope Glycoproteins Induce the Production of TNF-α and IL-10 in Human Monocytes by Activating Calcium Pathway. Sci Rep. 2018;8(1):17215.
69. Olivetta E, Percario Z, Fiorucci G, Mattia G, Schiavoni I, Dennis C, et al. HIV-1 Nef induces the release of inflammatory factors from human

monocyte/macrophages: involvement of Nef endocytotic signals and NF-kappa B activation. J Immunol. 2003;170(4):1716-27.

70. Henrick BM, Yao XD, Rosenthal KL, team Is. HIV-1 Structural Proteins Serve as PAMPs for TLR2 Heterodimers Significantly Increasing Infection and Innate Immune Activation. Front Immunol. 2015;6:426.

71. Asensio VC, Maier J, Milner R, Boztug K, Kincaid C, Moulard M, et al. Interferon-independent, human immunodeficiency virus type 1 gp120-mediated induction of CXCL10/IP-10 gene expression by astrocytes in vivo and in vitro. J Virol. 2001;75(15):7067-77.

72. Kutsch O, Oh J, Nath A, Benveniste EN. Induction of the chemokines interleukin-8 and IP-10 by human immunodeficiency virus type 1 tat in astrocytes. J Virol. 2000;74(19):9214-21.

73. Piatak M, Saag MS, Yang LC, Clark SJ, Kappes JC, Luk KC, et al. High levels of HIV-1 in plasma during all stages of infection determined by competitive PCR. Science. 1993;259(5102):1749-54.

74. Fiebig EW, Wright DJ, Rawal BD, Garrett PE, Schumacher RT, Peddada L, et al. Dynamics of HIV viremia and antibody seroconversion in plasma donors: implications for diagnosis and staging of primary HIV infection. AIDS. 2003;17(13):1871-9.

75. Gray ER, Bain R, Varsaneux O, Peeling RW, Stevens MM, McKendry RA. p24 revisited: a landscape review of antigen detection for early HIV diagnosis. AIDS. 2018;32(15):2089-102.

76. Schüpbach J, Böni J. Quantitative and sensitive detection of immune-complexed and free HIV antigen after boiling of serum. J Virol Methods. 1993;43(2):247-56.

77. Lillo FB, Cao Y, Concedi DR, Varnier OE. Improved detection of serum HIV p24 antigen after acid dissociation of immune complexes. AIDS. 1993;7(10):1331-6.

78. Read JS, Rich KC, Korelitz JJ, Mofenson LM, Harris R, Moye JH, et al. Quantification of human immunodeficiency virus type 1 p24 antigen and antibody rivals human immunodeficiency virus type 1 RNA and CD4+ enumeration for prognosis. National Institute of Child Health and Human Development Intravenous Immunoglobulin Clinical Trial Study Group. Pediatr Infect Dis J. 2000;19(6):544-51.

79. Morand-Joubert L, Costagliola D, Bludau H, Petit JC, Lefrère JJ. Predicting progression of HIV disease: usefulness of acid-dissociated p24 antigen. J Acquir Immune Defic Syndr (1988). 1994;7(7):676-80.
80. Sterling TR, Hoover DR, Astemborski J, Vlahov D, Bartlett JG, Schupbach J. Heat-denatured human immunodeficiency virus type 1 protein 24 antigen: prognostic value in adults with early-stage disease. J Infect Dis. 2002;186(8):1181-5.
81. Farzadegan H, Henrard DR, Kleeberger CA, Schrager L, Kirby AJ, Saah AJ, et al. Virologic and serologic markers of rapid progression to AIDS after HIV-1 seroconversion. J Acquir Immune Defic Syndr Hum Retrovirol. 1996;13(5):448-55.
82. Ledergerber B, Flepp M, Böni J, Tomasik Z, Cone RW, Lüthy R, et al. Human immunodeficiency virus type 1 p24 concentration measured by boosted ELISA of heat-denatured plasma correlates with decline in CD4 cells, progression to AIDS, and survival: comparison with viral RNA measurement. J Infect Dis. 2000;181(4):1280-8.
83. Schüpbach J. Viral RNA and p24 antigen as markers of HIV disease and antiretroviral treatment success. Int Arch Allergy Immunol. 2003;132(3):196-209.
84. Orlandi C, Canovari B, Bozzano F, Marras F, Pasquini Z, Barchiesi F, et al. A comparative analysis of unintegrated HIV-1 DNA measurement as a potential biomarker of the cellular reservoir in the blood of patients controlling and non-controlling viral replication. J Transl Med. 2020;18(1):204.
85. Surdo M, Cortese MF, Orlandi C, Di Santo F, Aquaro S, Magnani M, et al. Different kinetics of viral replication and DNA integration in the main HIV-1 cellular reservoirs in the presence and absence of integrase inhibitors. Antiviral Res. 2018;160:165-74.
86. Casabianca A, Orlandi C, Canovari B, Scotti M, Acetoso M, Valentini M, et al. A real time PCR platform for the simultaneous quantification of total and extrachromosomal HIV DNA forms in blood of HIV-1 infected patients. PLoS One. 2014;9(11):e111919.
87. Kamat A, Misra V, Cassol E, Ancuta P, Yan Z, Li C, et al. A plasma biomarker signature of immune activation in HIV patients on antiretroviral therapy. PLoS One. 2012;7(2):e30881.

88. Keating SM, Golub ET, Nowicki M, Young M, Anastos K, Crystal H, et al. The effect of HIV infection and HAART on inflammatory biomarkers in a population-based cohort of women. AIDS. 2011;25(15):1823-32.
89. Lei J, Yin X, Shang H, Jiang Y. IP-10 is highly involved in HIV infection. Cytokine. 2019;115:97-103.
90. Mhandire K, Mlambo T, Zijenah LS, Duri K, Mateveke K, Tshabalala M, et al. Plasma IP-10 Concentrations Correlate Positively with Viraemia and Inversely with CD4 Counts in Untreated HIV Infection. Open AIDS J. 2017;11:24-31.
91. Valverde-Villegas JM, de Medeiros RM, Ellwanger JH, Santos BR, Melo MG, Almeida SEM, et al. High CXCL10/IP-10 levels are a hallmark in the clinical evolution of the HIV infection. Infect Genet Evol. 2018;57:51-8.
92. Ploquin MJ, Madec Y, Casrouge A, Huot N, Passaes C, Lécuroux C, et al. Elevated Basal Pre-infection CXCL10 in Plasma and in the Small Intestine after Infection Are Associated with More Rapid HIV/SIV Disease Onset. PLoS Pathog. 2016;12(8):e1005774.
93. Mooney S, Tracy R, Osler T, Grace C. Elevated Biomarkers of Inflammation and Coagulation in Patients with HIV Are Associated with Higher Framingham and VACS Risk Index Scores. PLoS One. 2015;10(12):e0144312.
94. Williams B, Livak B, Bahk M, Keating SM, Adeyemi OM. Short Communication: SCD14 and SCD163 Levels Are Correlated with VACS Index Scores: Initial Data from the Blunted Immune Recovery in CORE Patients with HIV (BIRCH) Cohort. AIDS Res Hum Retroviruses. 2016;32(2):144-7.
95. Liu M, Guo S, Hibbert JM, Jain V, Singh N, Wilson NO, et al. CXCL10/IP-10 in infectious diseases pathogenesis and potential therapeutic implications. Cytokine Growth Factor Rev. 2011;22(3):121-30.
96. Jiao Y, Zhang T, Wang R, Zhang H, Huang X, Yin J, et al. Plasma IP-10 is associated with rapid disease progression in early HIV-1 infection. Viral Immunol. 2012;25(4):333-7.
97. Liovat AS, Rey-Cuillé MA, Lécuroux C, Jacquelin B, Girault I, Petitjean G, et al. Acute plasma biomarkers of T cell activation set-point levels and of disease progression in HIV-1 infection. PLoS One. 2012;7(10):e46143.

98. Noel N, Lerolle N, Lécuroux C, Goujard C, Venet A, Saez-Cirion A, et al. Immunologic and Virologic Progression in HIV Controllers: The Role of Viral "Blips" and Immune Activation in the ANRS CO21 CODEX Study. PLoS One. 2015;10(7):e0131922.
99. Riitho V, Connon R, Gwela A, Namusanje J, Nhema R, Siika A, et al. Biomarkers of mortality in adults and adolescents with advanced HIV in sub-Saharan Africa. Nat Commun. 2024;15(1):5492.
100. Freeman ML, Hossain MB, Burrowes SAB, Jeudy J, Bui R, Moisi D, et al. Association of Soluble Markers of Inflammation With Peri-coronary Artery Inflammation in People With and Without HIV Infection and Without Cardiovascular Disease. Open Forum Infect Dis. 2023;10(8):ofad328.
101. Oikonomou EK, Marwan M, Desai MY, Mancio J, Alashi A, Hutt Centeno E, et al. Non-invasive detection of coronary inflammation using computed tomography and prediction of residual cardiovascular risk (the CRISP CT study): a post-hoc analysis of prospective outcome data. Lancet. 2018;392(10151):929-39.
102. van den Borne P, Quax PH, Hoefer IE, Pasterkamp G. The multifaceted functions of CXCL10 in cardiovascular disease. Biomed Res Int. 2014;2014:893106.
103. Szentes V, Gazdag M, Szokodi I, Dézsi CA. The Role of CXCR3 and Associated Chemokines in the Development of Atherosclerosis and During Myocardial Infarction. Front Immunol. 2018;9:1932.
104. Heller EA, Liu E, Tager AM, Yuan Q, Lin AY, Ahluwalia N, et al. Chemokine CXCL10 promotes atherogenesis by modulating the local balance of effector and regulatory T cells. Circulation. 2006;113(19):2301-12.
105. Domingo P, Mateo MG, Villarroya J, Cereijo R, Torres F, Domingo JC, et al. Increased Circulating Levels of Growth Differentiation Factor 15 in Association with Metabolic Disorders in People Living with HIV Receiving Combined Antiretroviral Therapy. J Clin Med. 2022;11(3).
106. Debroy P, Pike F, Gawrieh S, Corey KE, Hartig S, Balasubramanyam A, et al. Circulating fibroblast growth factor 21 and growth differentiation factor 15 are associated with severity of hepatic steatosis in people with HIV. HIV Med. 2025;26(9):1457-62.

107. Boustani A, Ford MK, Kulbe JR, Laird AE, Shu L, Spencer M, et al. Increased Growth Differentiation Factor 15 Levels Are Associated with HIV-Associated Neurocognitive Impairment: A Pilot Study. Brain Sci. 2025;15(1).
108. Royston L, Isnard S, Perrin N, Sinyavskaya L, Berini C, Lin J, et al. Growth differentiation factor-15 as a biomarker of atherosclerotic coronary plaque: Value in people living with and without HIV. Front Cardiovasc Med. 2022;9:964650.
109. Secemsky EA, Scherzer R, Nitta E, Wu AH, Lange DC, Deeks SG, et al. Novel Biomarkers of Cardiac Stress, Cardiovascular Dysfunction, and Outcomes in HIV-Infected Individuals. JACC Heart Fail. 2015;3(8):591-9.
110. Barletta JM, Edelman DC, Constantine NT. Lowering the detection limits of HIV-1 viral load using real-time immuno-PCR for HIV-1 p24 antigen. Am J Clin Pathol. 2004;122(1):20-7.
111. Kim EY, Stanton J, Korber BT, Krebs K, Bogdan D, Kunstman K, et al. Detection of HIV-1 p24 Gag in plasma by a nanoparticle-based bio-barcode-amplification method. Nanomedicine (Lond). 2008;3(3):293-303.
112. Passaes CPB, Bruel T, Decalf J, David A, Angin M, Monceaux V, et al. Ultrasensitive HIV-1 p24 Assay Detects Single Infected Cells and Differences in Reservoir Induction by Latency Reversal Agents. J Virol. 2017;91(6).
113. Kuzmichev YV, Lackman-Smith C, Bakkour S, Wiegand A, Bale MJ, Musick A, et al. Application of ultrasensitive digital ELISA for p24 enables improved evaluation of HIV-1 reservoir diversity and growth kinetics in viral outgrowth assays. Sci Rep. 2023;13(1):10958.
114. Levinger C, Howard JN, Cheng J, Tang P, Joshi A, Catalfamo M, et al. An ultrasensitive planar array p24 Gag ELISA to detect HIV-1 in diverse biological matrixes. Sci Rep. 2021;11(1):23682.
115. Scully EP, Gandhi M, Johnston R, Hoh R, Lockhart A, Dobrowolski C, et al. Sex-Based Differences in Human Immunodeficiency Virus Type 1 Reservoir Activity and Residual Immune Activation. J Infect Dis. 2019;219(7):1084-94.
116. Meditz AL, Folkvord JM, Lyle NH, Searls K, Lie YS, Coakley EP, et al. CCR5 expression is reduced in lymph nodes of HIV type 1-infected women, compared with men, but does not mediate sex-based differences in viral loads. J Infect Dis. 2014;209(6):922-30.

117. Das B, Dobrowolski C, Luttge B, Valadkhan S, Chomont N, Johnston R, et al. Estrogen receptor-1 is a key regulator of HIV-1 latency that imparts gender-specific restrictions on the latent reservoir. Proc Natl Acad Sci U S A. 2018;115(33):E7795-E804.
118. Abdel-Mohsen M, Richman D, Siliciano RF, Nussenzweig MC, Howell BJ, Martinez-Picado J, et al. Recommendations for measuring HIV reservoir size in cure-directed clinical trials. Nat Med. 2020;26(9):1339-50.
119. Petitjean G, Al Tabaa Y, Tuaillon E, Mettling C, Baillat V, Reynes J, et al. Unintegrated HIV-1 provides an inducible and functional reservoir in untreated and highly active antiretroviral therapy-treated patients. Retrovirology. 2007;4:60.
120. Ramratnam B, Mittler JE, Zhang L, Boden D, Hurley A, Fang F, et al. The decay of the latent reservoir of replication-competent HIV-1 is inversely correlated with the extent of residual viral replication during prolonged anti-retroviral therapy. Nat Med. 2000;6(1):82-5.
121. Maldarelli F, Palmer S, King MS, Wiegand A, Polis MA, Mican J, et al. ART suppresses plasma HIV-1 RNA to a stable set point predicted by pretherapy viremia. PLoS Pathog. 2007;3(4):e46.
122. Tosiano MA, Jacobs JL, Shutt KA, Cyktor JC, Mellors JW. A Simpler and More Sensitive Single-Copy HIV-1 RNA Assay for Quantification of Persistent HIV-1 Viremia in Individuals on Suppressive Antiretroviral Therapy. J Clin Microbiol. 2019;57(3).
123. Darcis G, Maes N, Pasternak AO, Sauvage AS, Frippiat F, Meuris C, et al. Detectability of HIV Residual Viremia despite Therapy Is Highly Associated with Treatment with a Protease Inhibitor-Based Combination Antiretroviral Therapy. Antimicrob Agents Chemother. 2020;64(3).
124. Schüpbach J. Measurement of HIV-1 p24 antigen by signal-amplification-boosted ELISA of heat-denatured plasma is a simple and inexpensive alternative to tests for viral RNA. AIDS Rev. 2002;4(2):83-92.
125. Ribas SG, Ondoa P, Schüpbach J, van der Groen G, Fransen K. Performance of a quantitative human immunodeficiency virus type 1 p24 antigen assay on various HIV-1 subtypes for the follow-up of human immunodeficiency type 1 seropositive individuals. J Virol Methods. 2003;113(1):29-34.

126. Simmons RP, Scully EP, Groden EE, Arnold KB, Chang JJ, Lane K, et al. HIV-1 infection induces strong production of IP-10 through TLR7/9-dependent pathways. AIDS. 2013;27(16):2505-17.
127. Gray CM, Hong HA, Young K, Lewis DA, Fallows D, Manca C, et al. Plasma interferon-gamma-inducible protein 10 can be used to predict viral load in HIV-1-infected individuals. J Acquir Immune Defic Syndr. 2013;63(3):e115-6.
128. Pastor L, Casellas A, Rupérez M, Carrillo J, Maculuve S, Jairoce C, et al. Interferon-γ-Inducible Protein 10 (IP-10) as a Screening Tool to Optimize Human Immunodeficiency Virus RNA Monitoring in Resource-Limited Settings. Clin Infect Dis. 2017;65(10):1670-5.
129. Wang Z, Yin X, Ma M, Ge H, Lang B, Sun H, et al. IP-10 Promotes Latent HIV Infection in Resting Memory CD4. Front Immunol. 2021;12:656663.
130. Lee S, Chung YS, Yoon CH, Shin Y, Kim S, Choi BS, et al. Interferon-inducible protein 10 (IP-10) is associated with viremia of early HIV-1 infection in Korean patients. J Med Virol. 2015;87(5):782-9.
131. Blazkova J, Whitehead EJ, Schneck R, Shi V, Justement JS, Rai MA, et al. Immunologic and Virologic Parameters Associated With Human Immunodeficiency Virus (HIV) DNA Reservoir Size in People With HIV Receiving Antiretroviral Therapy. J Infect Dis. 2024;229(6):1770-80.
132. Chéret A, Durier C, Mélard A, Ploquin M, Heitzmann J, Lécuroux C, et al. Impact of early cART on HIV blood and semen compartments at the time of primary infection. PLoS One. 2017;12(7):e0180191.
133. Lane BR, King SR, Bock PJ, Strieter RM, Coffey MJ, Markovitz DM. The C-X-C chemokine IP-10 stimulates HIV-1 replication. Virology. 2003;307(1):122-34.
134. Cameron PU, Saleh S, Sallmann G, Solomon A, Wightman F, Evans VA, et al. Establishment of HIV-1 latency in resting CD4+ T cells depends on chemokine-induced changes in the actin cytoskeleton. Proc Natl Acad Sci U S A. 2010;107(39):16934-9.
135. Hardaker EL, Bacon AM, Carlson K, Roshak AK, Foley JJ, Schmidt DB, et al. Regulation of TNF-alpha- and IFN-gamma-induced CXCL10 expression: participation of the airway smooth muscle in the pulmonary inflammatory response in chronic obstructive pulmonary disease. FASEB J. 2004;18(1):191-3.

136. Williams R, Dhillon NK, Hegde ST, Yao H, Peng F, Callen S, et al. Proinflammatory cytokines and HIV-1 synergistically enhance CXCL10 expression in human astrocytes. Glia. 2009;57(7):734-43.